

DESCRIBING THE PLATYCOSMS

J. H. CONWAY[†] AND J. P. ROSSETTI[‡]

ABSTRACT. We study in detail the closed flat Riemannian 3-manifolds.

CONTENTS

1. Introduction	1
2. Dimension 2	2
3. Picturing the Platycosms - Space Groups	4
4. Parameters for Platycosms	11
5. Embedded Flat Surfaces	16
6. Infinite Platycosms	19
7. Fundamental Groups, Homology and Automorphisms	22
8. Double Covers	28
9. Diameters and Injectivity Radii	30
10. Some Formulae for Torocosms and Lattices	34
11. The Bravais-Voronoi Classes	35
Appendix I: Why there are just 10 platycosms	39
Appendix II: Conorms of Lattices	42
Appendix III: Dictionary of Names and Notations	44
References	46

1. INTRODUCTION

That there are just 10 closed flat 3-manifolds — we propose to call them *platycosms* — has been known since around 1933. Since then, they have been studied in many papers and several books, for example [Th], [We1], [Wo]. They are of interest to speculative physicists as well as mathematicians, and indeed there are some recent astronomical observations that suggest that the physical universe might actually be a platycosm! (see for example [E], [HS], [NYT], [Spe], [TOH], [URLW]).

We believe that these 10 manifolds should be more widely known. Accordingly, our principal aim in this paper is to give a complete discussion of the ten compact platycosms. In particular, we give them a uniform set of individual names, specify

2000 *Mathematics Subject Classification*. 20F34, 57S30, 20H15.

Key words and phrases. Platycosm, flat manifold, space group, automorphism, lattice, Bravais, Voronoi, cover, diameter.

[†] NSF grant DMS-0072839. [‡] Supported by a Guggenheim fellowship.

parameters in a systematic way, and give presentations for their fundamental groups, which we use to derive their homology groups, automorphism groups and list their double covers.

We then study their geometry, finding their Bravais types, diameters and injectivity radii, and listing the compact embedded flat surfaces.

We have also included brief treatments of some related topics, namely the 2-dimensional analogues of the platycosms, the 8 infinite platycosms and the 219 crystallographic groups.

Appendix I gives a brief proof that the list of 10 is complete, Appendix II describes the “conorms” we use as parameters, while Appendix III is a dictionary between our names and others.

An accompanying paper [RC] proves that, up to scale, there is a unique isospectral pair of platycosms, the ‘DDT-example’ of [DR].

Acknowledgements: We have benefitted from conversations with Jeff Weeks, Bill Thurston, and most particularly with Peter Doyle, who has also helped us in many other ways. J. P. Rossetti is grateful to the Mathematics Department of Princeton University for its hospitality during the writing of this paper.

2. DIMENSION 2

Although our main aim in this paper is to describe the platycosms or 3-dimensional flat manifolds, particularly, the compact ones, we briefly discuss their 2-dimensional analogues in this section.

The 2-dimensional flat manifolds. Everybody is familiar with the torus and Klein bottle. Each of these can be given various locally Euclidean metrics — that is to say, can be realized as a *flat* 2-manifold. We can see this by “rolling up” the Euclidean plane in various ways: one obtains the typical flat torus T_{ABC} by dividing the plane by a 2-dimensional lattice of translations (Figure 1) — this is mathematically more natural than identifying opposite sides of a parallelogram, since each lattice can be defined by many different parallelograms. Beware: the parameters A, B, C for the torus are the negatives of the inner products of $\mathbf{w}, \mathbf{x}, \mathbf{y}$, rather than their norms, which are $A + B, A + C, B + C$.

The most general flat Klein bottle K_B^A (Figure 1) can be obtained in a similar way by dividing the plane by the group generated by the translation through a vector \mathbf{x} with norm $N(\mathbf{x}) = \mathbf{x} \cdot \mathbf{x} = A$ together with a glide reflection based on an orthogonal vector \mathbf{y} of norm B .

Voronoi and Bravais types. The metric of a flat torus is determined by the shape of its translation lattice. Voronoi classified lattices by the topological type of their Voronoi cell, which is either hexagonal or rectangular, while Bravais classified them by their symmetries, which are controlled by the shape of the Delaunay cells. The lattice parameters ABC we recommend, called *conorms* (see Figure 1 and Appendix II), easily yield both classifications (Table 1), since the Voronoi cell is rectangular just if some conorm vanishes, while the shape of the Delaunay cell is determined by this and which conorms are equal.

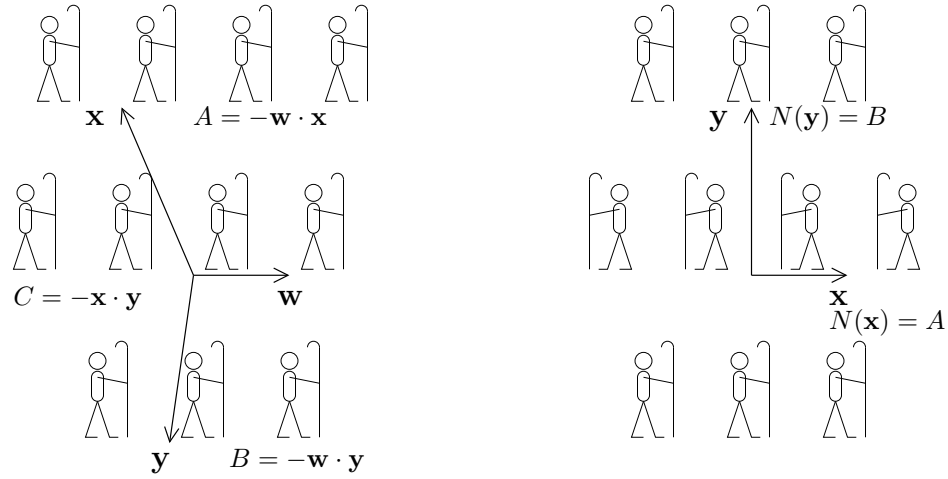


FIGURE 1. The torus T_{ABC} and the Klein bottle K_B^A .

conorms	topological type of Voronoi cell	shape of Delaunay cell	lattice shape
ABC	hexagonal	scalene triangle	generic lattice
$AA B$		isosceles triangle	rhombic lattice
AAA		equilateral triangle	hexagonal lattice
$AB 0$	rectangular	rectangle	rectangular lattice
$AA 0$		square	square lattice

TABLE 1. (it is understood that A, B, C are distinct and non-zero.)

If one lattice can be continuously deformed into another without changing either its Bravais or its Voronoi class, we say they are in the same ‘BraVo’ class¹

All these classifications can be applied to arbitrary flat manifolds and we discuss them for the platycosms in Section 11. All flat Klein bottles K_B^A lie in a single BraVo class since A and B can be continuously and independently varied through all positive values.

Infinite flat 2-manifolds. The torus and Klein bottle are finite 2-manifolds — that is to say, they have finite volume, or (equivalently for flat manifolds) are compact. There also exist just three types of infinite (or non-compact) flat 2-manifolds without boundary, namely the

- Euclidean Plane* $\mathbb{R}^2 (\cong T_{\infty\infty} = K_{\infty}^{\infty})$,
- (infinite) Cylinder* $C_A (\cong T_{A\infty} \cong K_{\infty}^A)$,
- Möbius Cylinder* $M_B (\cong K_B^{\infty})$,

¹This is not the same as saying that they are in the same Bravais class and also the same Voronoi class. The rhombic lattices $\Lambda_{AA B}$ split into two BraVo classes according as $A > B$ or $A < B$, between which we cannot pass without encountering a hexagonal lattice Λ_{AAA} .

illustrated in Figures 2 and 3. Their 3-dimensional analogues are discussed in Section 6.

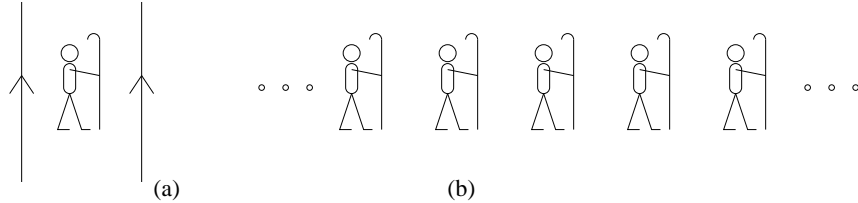


FIGURE 2. The (infinite) cylinder (a) and its covering plane (b).

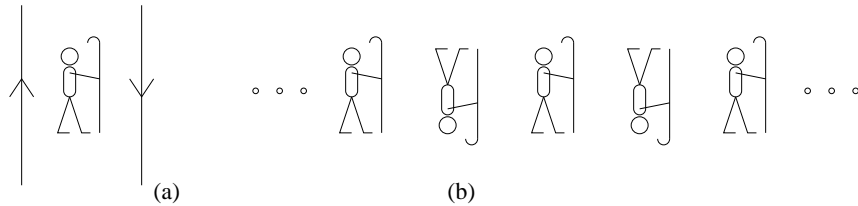


FIGURE 3. The Möbius cylinder (a) and its covering plane (b).

2-dimensional flat orbifolds. Dividing a Euclidean space by a discrete subgroup of its symmetries yields a manifold only when the group is *fixed-point-free* (i.e., only the identity element fixes any point of the space), or equivalently, *torsion-free* (i.e., only the identity element has finite order). More generally, one obtains a *flat orbifold*. There are just 17 types of compact flat 2-dimensional orbifolds, corresponding to the 17 plane crystallographic groups, which are called

*632, 632, *442, 4*2, 442, *333, 3*3, 333

*2222, 2*22, 22*, 22 \times , 2222, **, * \times , $\times\times$, \circ

in the orbifold notation [Co1], the last two being the Klein bottle and the torus. The analogous results in 3 dimensions are discussed in Section 3.

3. PICTURING THE PLATYCOSMS - SPACE GROUPS

We shall use the term *platycosm* (“flat universe”) for a compact locally Euclidean 3-manifold without boundary, since these are the simplest alternative universes for us to think of living in [LSW]. (The program *Curved Spaces* of Jeff Weeks — accompanying [We2] — allows you to ‘fly’ through platycosms and other spaces.) If you lived in a small enough platycosm, you would appear to be surrounded by images of yourself which can be arranged in one of ten essentially different ways (Figures 12, 13, 4(i), 4(ii), 15, 16, 5, 6, 18(i), 18(ii)).

The images one sees of oneself lie in the manifold’s universal cover, which is of course a Euclidean 3-space \mathbb{R}^3 . The symmetry operators that relate them form

a crystallographic space-group Γ , and geometrically the manifold is the quotient space \mathbb{R}^3/Γ .

If you hold something in one hand, your images will either all hold things with the same hand (if the manifold is orientable, Figures 4, 12, 15, 16) or half with

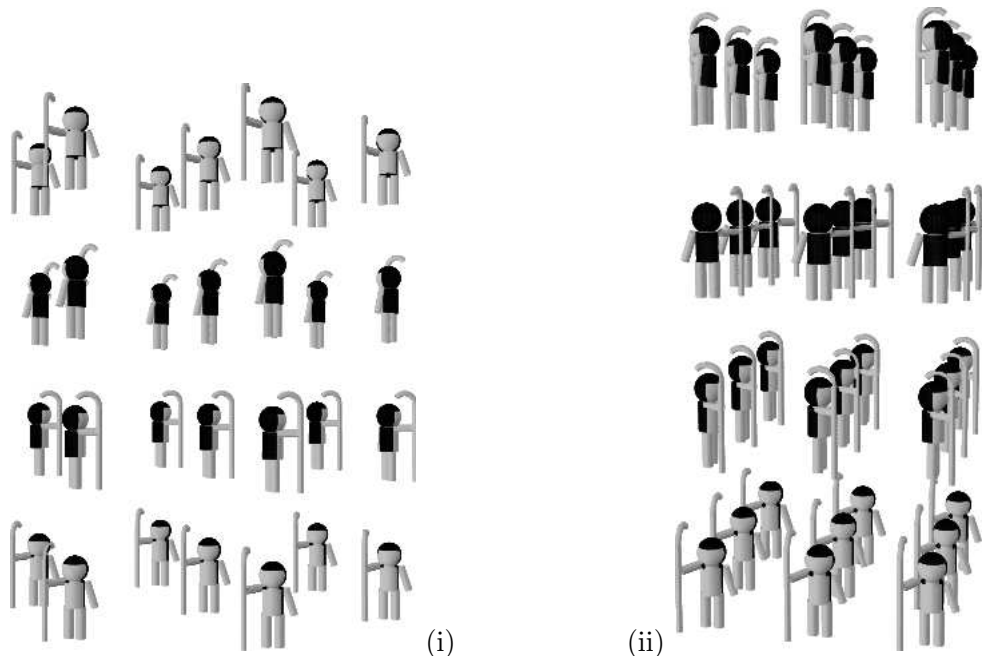


FIGURE 4. (i) a tricasm, and (ii) a tetracosm.

their left hand and half with their right (if not; Figures 5, 6, 18). We therefore call a platycosm *chiral* (“handed”) or *amphichiral* (“either handed”) according as it is or is not orientable. Selecting the images of a particular handedness in the picture for a non-orientable manifold X yields the picture for its orientable double cover, Y , so we regard X as an ‘amphichiralized’ version of Y , and call it ‘an amphi- Y ’.

The chiral platycosms are the *helicosms* $c1, c2, c3, c4, c6$ (individually called the *torocosm, dicosm, tricasm, tetracosm, hexacosm*) and the *didicosm* $c22$, also known as the *Hantzsche-Wendt manifold*. In these notations, the letter “ c ” stands for “chiral” while the digits indicate the point group, which is a cyclic group C_N of order N for cN , and $C_2 \times C_2$ for $c22$.

A *torocosm* (usually called a 3-torus) is just the 3-dimensional analogue of a torus. The space group for another helicosm cN is generated by a suitable 2-dimensional lattice of translations together with an orthogonal screw motion of period² N , while the space group for a didicosm is generated by orthogonal period 2 screw motions whose axes bisect the faces of a ‘box’ as in Figure 7. The space is tessellated into such boxes.

²We say a screw motion has period N if the lowest power of it that is a translation is the N^{th} .

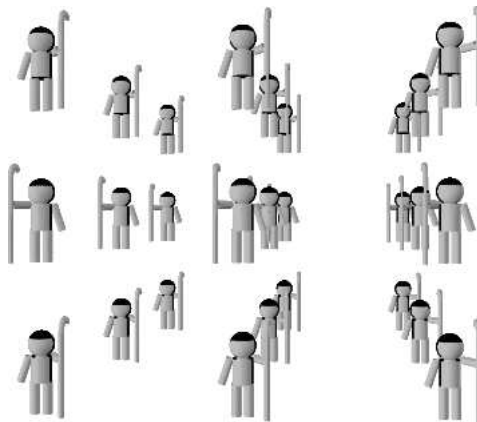
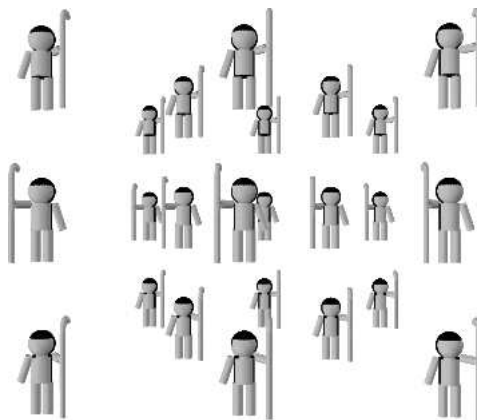
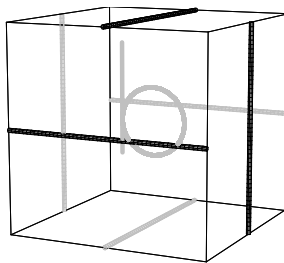
FIGURE 5. A first ampicosm $+a1$.FIGURE 6. A second ampicosm $-a1$.

FIGURE 7. The didicosm space group is generated by the half-turn screw motions corresponding to the indicated lines.

The amphichiral platycosms are the *first* and *second* (or *positive* and *negative*) *ampicosms*, $\pm a1$, and *amphidicosms*, $\pm a2$, whose orientable double covers are $c1$ and $c2$ respectively (Figures 5, 6, 18). The figures become easier to follow if

we replace the human bodies (of Fig. 6, say) by boxes bearing the letters **b,d,p,q** and insert some labelled **o** to indicate spacing (as in Fig. 8).

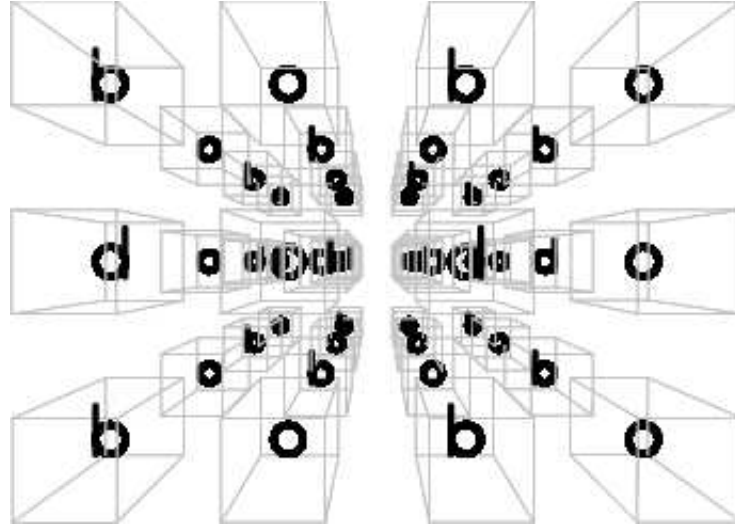


FIGURE 8. Another picture of a second amphicosm.

Such shorter figures for the amphis (Fig. 9) abbreviate nicely to

$$(1) \quad \begin{array}{|c|c|} \hline \mathbf{b} & \mathbf{o} \\ \hline \mathbf{d} & \mathbf{o} \\ \hline \end{array} \begin{array}{|c|c|} \hline \mathbf{b} & \mathbf{o} \\ \hline \mathbf{d} & \mathbf{o} \\ \hline \end{array} \quad \begin{array}{|c|c|} \hline \mathbf{b} & \mathbf{o} \\ \hline \mathbf{d} & \mathbf{o} \\ \hline \end{array} \begin{array}{|c|c|} \hline \mathbf{o} & \mathbf{b} \\ \hline \mathbf{o} & \mathbf{d} \\ \hline \end{array} \quad \begin{array}{|c|c|} \hline \mathbf{b} & \mathbf{o} \\ \hline \mathbf{d} & \mathbf{o} \\ \hline \end{array} \begin{array}{|c|c|} \hline \mathbf{p} & \mathbf{o} \\ \hline \mathbf{q} & \mathbf{o} \\ \hline \end{array} \quad \begin{array}{|c|c|} \hline \mathbf{b} & \mathbf{o} \\ \hline \mathbf{d} & \mathbf{o} \\ \hline \end{array} \begin{array}{|c|c|} \hline \mathbf{o} & \mathbf{p} \\ \hline \mathbf{o} & \mathbf{q} \\ \hline \end{array}$$

$+a1 \qquad -a1 \qquad +a2 \qquad -a2$

in which it is understood that the letters continue with period two in all directions. Their space groups consist precisely of the operations that take the leading box labelled ‘**b**’ to the other boxes labelled **b, d, p** or **q**.

We chose these standard forms because when x and y are orthogonal the first amphicosm is the Cartesian product of a Klein bottle and circle (in later notation: $+a1_{A:B}^D = K_A^D \times S_B^1$). However, they can be continuously deformed into the *variant forms*:

$$(2) \quad \begin{array}{|c|c|} \hline \mathbf{b} & \mathbf{o} \\ \hline \mathbf{d} & \mathbf{o} \\ \hline \end{array} \begin{array}{|c|c|} \hline \mathbf{d} & \mathbf{o} \\ \hline \mathbf{b} & \mathbf{o} \\ \hline \end{array} \quad \begin{array}{|c|c|} \hline \mathbf{b} & \mathbf{o} \\ \hline \mathbf{d} & \mathbf{o} \\ \hline \end{array} \begin{array}{|c|c|} \hline \mathbf{o} & \mathbf{d} \\ \hline \mathbf{o} & \mathbf{b} \\ \hline \end{array} \quad \begin{array}{|c|c|} \hline \mathbf{b} & \mathbf{o} \\ \hline \mathbf{d} & \mathbf{o} \\ \hline \end{array} \begin{array}{|c|c|} \hline \mathbf{q} & \mathbf{o} \\ \hline \mathbf{p} & \mathbf{o} \\ \hline \end{array} \quad \begin{array}{|c|c|} \hline \mathbf{b} & \mathbf{o} \\ \hline \mathbf{d} & \mathbf{o} \\ \hline \end{array} \begin{array}{|c|c|} \hline \mathbf{o} & \mathbf{q} \\ \hline \mathbf{o} & \mathbf{p} \\ \hline \end{array}$$

$+a1 \qquad -a1 \qquad +a2 \qquad -a2$

in necessarily two different ways. For the amphicosms, one can use the ‘shear motion’ that lifts each layer ‘one-half a unit’ more than the one in front of it (or, in later notation, just change base from $\mathbf{x}, \mathbf{y}, \mathbf{z}$ to $\mathbf{x}, \pm\mathbf{w}, \mathbf{z}$). The amphidicosms need only the ‘shift of motif’ that leaves the metric undisturbed, but moves each

letter half way to the one above (in the **b, d** layers) or below it (in the **p, q** ones). The variant forms are more useful in determining fundamental groups and automorphisms.

A similar figure for the didicosm is

$$(3) \quad c22 : \begin{array}{|c|c|} \hline \mathbf{b} & \circ \\ \hline \circ & \mathbf{d} \\ \hline \end{array} \begin{array}{|c|c|} \hline \circ & \mathbf{p} \\ \hline \mathbf{q} & \circ \\ \hline \end{array}$$

in which the non-bold letters are those seen from behind, through the boxes (Figure 10).

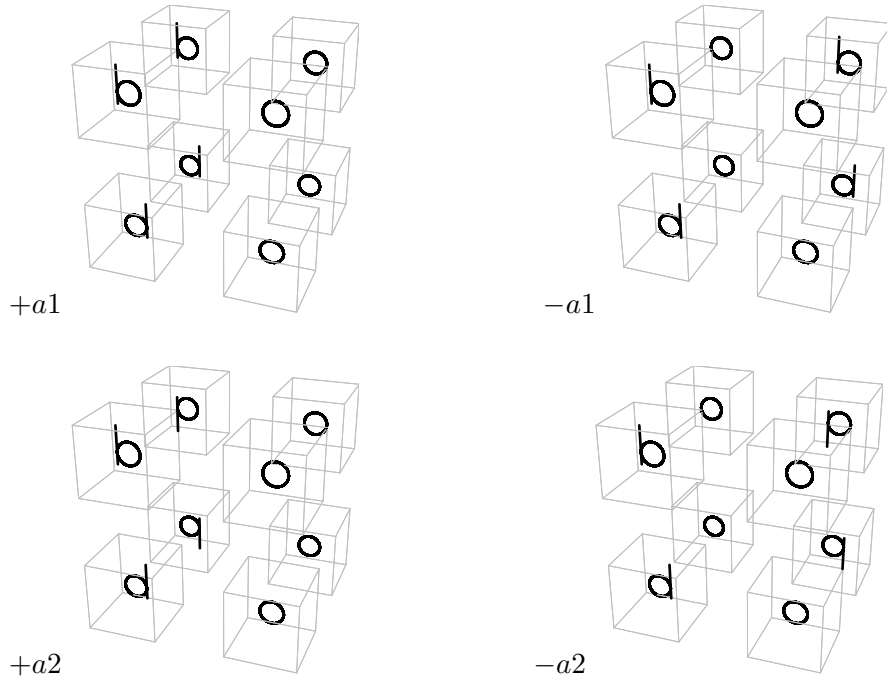


FIGURE 9. The ampicosms $\pm a1$ and the amphidicosms $\pm a2$.

Platycosms and space groups. Why are there only 10 platycosms? The real reason is that just 10 of the crystallographic space groups are fixed-point-free, analogously to the two plane crystallographic groups \circ and $\times\times$ that yield the torus and Klein bottle. In fact, Nowacki [No] found the 10 compact platycosms in 1934 by finding which of the space groups of the International list were fixed-point-free. A new and simple enumeration of the 219 space groups is given in [CDHT], from which one can easily read off the numbers having various properties (and so, in particular, pick out the platycosms). Of course one can obtain a much shorter enumeration by restricting the argument to platycosms throughout, as was done by Hantzsche and Wendt [HW] in 1934. We give a simpler proof of this type in Appendix I.

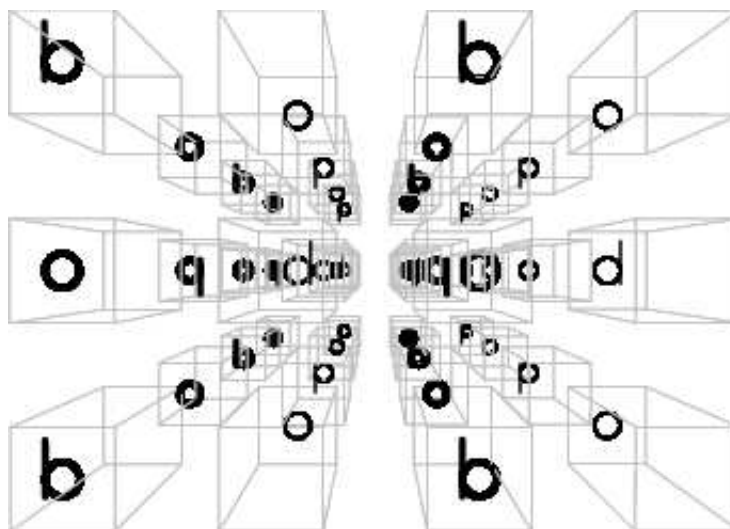


FIGURE 10. A didicosm $c22$.

# parameters	1	2	3	4	6	#
# fibrations	0	1	3	∞	∞	-
total	35_0	110_1	$12_1 + 26_2 + 21_3$	$5_2 + 8_3$	2_1	219
chiral	12_0	29_1	$5_1 + 4_2$	$2_2 + 1_3$	1_1	54
metachiral	1	10	0	0	0	11
point groups in this case	*432, 432 *332, 3*2 332	*22N, 22N *NN, N*, NN 2*M, M*	*222, 222, *22	2*, 22, *	$\times, 1$	-
# pt. groups	5	19	3	3	2	32

# parameters	2	3	4	6	#
platycosms	$c3, c4, c6$	$c22, \pm a2$	$c2, \pm a1$	$c1$	10
# fibrations	1	3	∞	∞	-
total	3_1	$1_1 + 2_3$	$1_2 + 2_3$	1_1	10
chiral	3_1	1_1	1_2	1_1	6
metachiral	3	0	0	0	3
point groups	33, 44, 66	222, *22	22, *	1	
# pt. groups	3	2	2	1	8

TABLE 2. The upper table arranges space groups according to their point groups and numbers of parameters and Seifert fibrations. The lower table restricts this information to platycosms. The number M is 2 or 3, and N is 3 or 4 or 6.

We briefly describe the terms used here. A space-group is *amphichiral* (“either handed”) or *achiral* (“not handed”)³ if it contains handedness-reversing operations; otherwise it is *chiral* (“handed”). It is *metachiral* if the group itself is distinct from its mirror image.

³The terms “chiral” and “achiral” were introduced by Lord Kelvin before 1896, when he used them in his Baltimore Lectures. Coxeter’s enlargement of the latter to *amphichiral* avoids using the negating prefix for a positive property.

The *point group* is the group obtained by identifying any two elements of the space group that differ by a translation. We specify these finite crystallographic groups in the orbifold notation [Co1]. The space groups with a given point group constitute one of the 32 *crystal classes*.

The number of space-groups is often given as 230, because the metachiral ones are counted twice, once for each of their two inequivalent orientations. From the orbifold point of view this way of counting is incorrect — it would wrongly make us say there were 13 platycosms! The numbers of types of oriented orbifolds and platycosms are only $54+11=65$ and $6+3 = 9$ rather than 219 and 13. The 9 oriented platycosm types arise as follows: the cases $\pm a1, \pm a2$, are non-orientable, so yield no oriented types; each of $c1, c2, c22$ has an orientation-reversing symmetry, so yields a single oriented type; finally $c3, c4, c6$ give two oriented types each, since for them the defining screw motion may be either *dextral* (like a corkscrew) or *sinistral* (like a reflected corkscrew).

Seifert fiber spaces. The orbifolds of many space groups can be realized as Seifert fiber spaces, the one-dimensional fibers being the images in the orbifold of a family of parallel lines that is fixed by the group. The number of such ‘Seifert fibrations’, if not 0 or 1, is at least 3 (in fact usually 3, otherwise ∞), since if two families of parallel lines are fixed so is the family of lines perpendicular to them⁴.

In Table 2, the numbers of cases with 3 or more fibrations appear with subscripts 1, 2 or 3 according as the fibrations are of 1, 2 or 3 distinct types. Thus the number with just three fibrations is given as $12_1 + 26_2 + 21_3$, meaning that there are 12 in which the three fibrations are all of 1 type, 26 in which the fibrations are of 2 distinct types, and 21 in which the fibrations are of 3 distinct types.

It happens that every platycosm has at least one realization as a Seifert fiber space. Each such fibration determines a plane crystallographic group (by “looking along the fibers”) and the “types” we now give (in Table 3) are the orbifold notations for these groups:

torocosm	$c1$	infinitely many fibrations, all of type \circ .
dicosm	$c2$	one fibration of type 2222, infinity of type $\times\times$.
tricosm	$c3$	one fibration of type 333.
tetracosm	$c4$	one fibration of type 444.
hexacosm	$c6$	one fibration of type 632.
didicosm	$c22$	just three fibrations, all of type $22\times$.
first amphicosm	$+a1$	one of type \circ , infinity of types $**$, $\times\times$.
second amphicosm	$-a1$	one of type \circ , infinity of types $**$, $\times\times$.
first amphidicosm	$+a2$	just three fibrations, of types $22*$, $**$, $\times\times$.
second amphidicosm	$-a2$	just three fibrations, of types $22\times$, $*\times$, $\times\times$.

TABLE 3. The platycosms and their Seifert fibrations.

⁴and this third family will be rationally related to the lattice if the first two are.

4. PARAMETERS FOR PLATYCOSMS

In the interest of consistency, the parameters we use are always the conorms of what we call the Naming lattice \mathcal{N} , generated by all the translation vectors, screw vectors, glide vectors. Since our parameters are often squared lengths, we introduce the convention that numbers inside a ‘square’ should be squared, for instance $c22^{\square abc}$ means $c22^{A^2 B^2 C^2}$, where $A = a^2$, $B = b^2$, $C = c^2$.

The Torocosm $c1_{ABC}^{DEF}$. This is our proposed name for the 3-dimensional torus. Geometrically it is the quotient \mathbb{R}^3/\mathcal{T} , where \mathcal{T} is the normal subgroup generated by translations — “the lattice of translations”. Our parameters A, B, \dots, F are the conorms (see Appendix II) of \mathcal{T} — in other words \mathcal{T} has an obtuse superbase $\mathbf{x}, \mathbf{y}, \mathbf{z}, \mathbf{t}$ with $\mathbf{y} \cdot \mathbf{z} = -A$, $\mathbf{z} \cdot \mathbf{x} = -B$, $\mathbf{x} \cdot \mathbf{y} = -C$, $\mathbf{x} \cdot \mathbf{t} = -D$, $\mathbf{y} \cdot \mathbf{t} = -E$, $\mathbf{z} \cdot \mathbf{t} = -F$. In the corresponding conorm diagram ((i) in Figure 11) the Voronoi vector corresponding to any line is a translation vector.

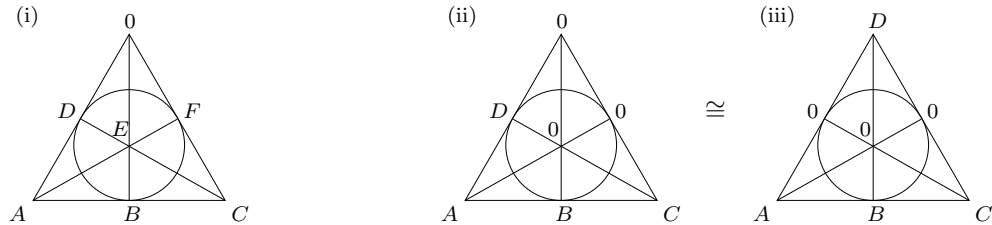


FIGURE 11. Conorms for Λ_{ABC}^{DEF} (i), and Λ_{ABC}^D (ii) and (iii).

We omit conorms with value 0: for instance the lattice for $c1_{ABC}^D$ has conorms (ii), or equivalently (iii) in Figure 11. The lattice for $c1^{ABC}$ is spanned by three orthogonal vectors of norms A, B, C as in Figure 12.

The torocosm is the helicocosm for $N = 1$. The N -cosms for $N = 2, 3, 4, 6$ (the other helicocosms) are generated by the translations of a 2-dimensional lattice $\langle \mathbf{w}, \mathbf{x}, \mathbf{y} \rangle$ where $\mathbf{w} + \mathbf{x} + \mathbf{y} = \mathbf{o}$, whose conorms are the lower parameters together with a period N screw motion along a perpendicular vector \mathbf{z} of norm D . The particular cases are:

The Dicosm $c2_{ABC}^D$. The 2-dimensional lattice Λ_{ABC} has an obtuse superbase of three vectors $\mathbf{w}, \mathbf{x}, \mathbf{y}$ with $\mathbf{w} + \mathbf{x} + \mathbf{y} = \mathbf{o}$ whose inner products $\mathbf{w} \cdot \mathbf{x} = -A$, $\mathbf{w} \cdot \mathbf{y} = -B$, $\mathbf{x} \cdot \mathbf{y} = -C$ are non-positive. The half turn negating all these vectors is an order 2 rotational symmetry. The space group for the dicosm $c2_{ABC}^D$ is generated by the translations of this lattice together with the period 2 screw motion obtained by combining the above rotation with a translation through a vector \mathbf{z} of norm D perpendicular to Λ_{ABC} , so the conorm function for the naming lattice Λ_{ABC}^D is (ii) or (iii) in Figure 11.

The Tricosm $c3_{AAA}^D$, **Tetracosm** $c4_{AAA}^D$, **Hexacosm** $c6_{AAA}^D$. Only certain special 2-dimensional lattices have higher order rotational symmetry. They are Λ_{AAA} which has order 3 and 6 rotations taking $\mathbf{w} \rightarrow \mathbf{x} \rightarrow \mathbf{y} \rightarrow \mathbf{w}$ and $\mathbf{w} \rightarrow$

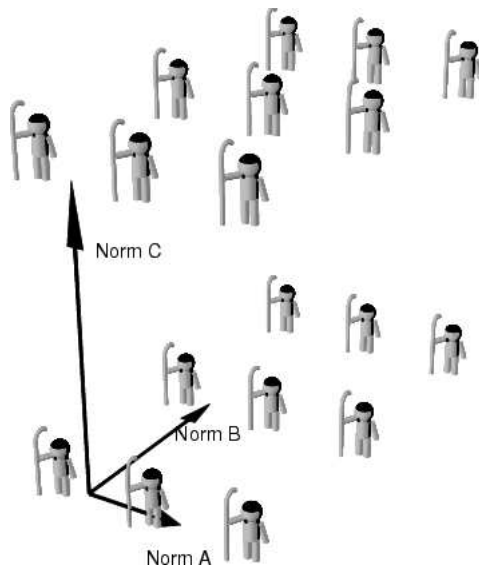
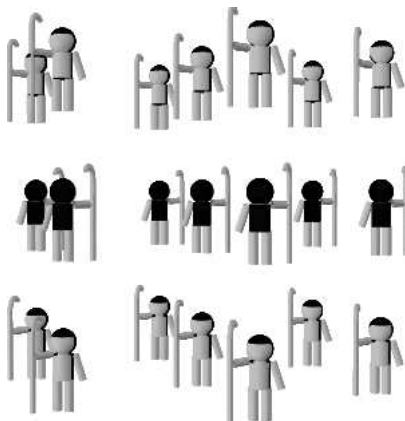
FIGURE 12. The orthogonal torocosm $c1^{ABC}$.

FIGURE 13. The dicosm.

$-\mathbf{y} \rightarrow \mathbf{x} \rightarrow -\mathbf{w}$ respectively (Figure 14 left), and Λ_{AA} (meaning Λ_{AA0}), which has the order 4 rotation $\mathbf{x} \rightarrow \mathbf{y} \rightarrow -\mathbf{x}$ (Figure 14 right).

The space groups of the tricostm $c3_{AAA}^D$ (Figure 4(i)), tetracosm $c4_{AA}^D$ (Figure 4(ii)), hexacosm $c6_{AAA}^D$ (Figure 15) are generated by the translations of the appropriate lattice together with the period 3, 4 or 6 screw motion obtained by combining the corresponding rotation with a translation through a perpendicular vector of norm D .

Since a period N screw motion with $N > 2$ is either *dextral* or *sinistral* (see Figure 15), the groups of these three manifolds have two enantiomorphic forms each — that is to say, they are metachiral.

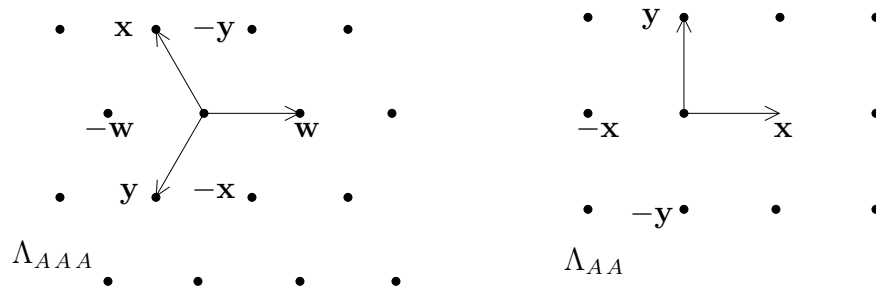


FIGURE 14. The hexagonal lattice Λ_{AAA} and square lattice Λ_{AA} .

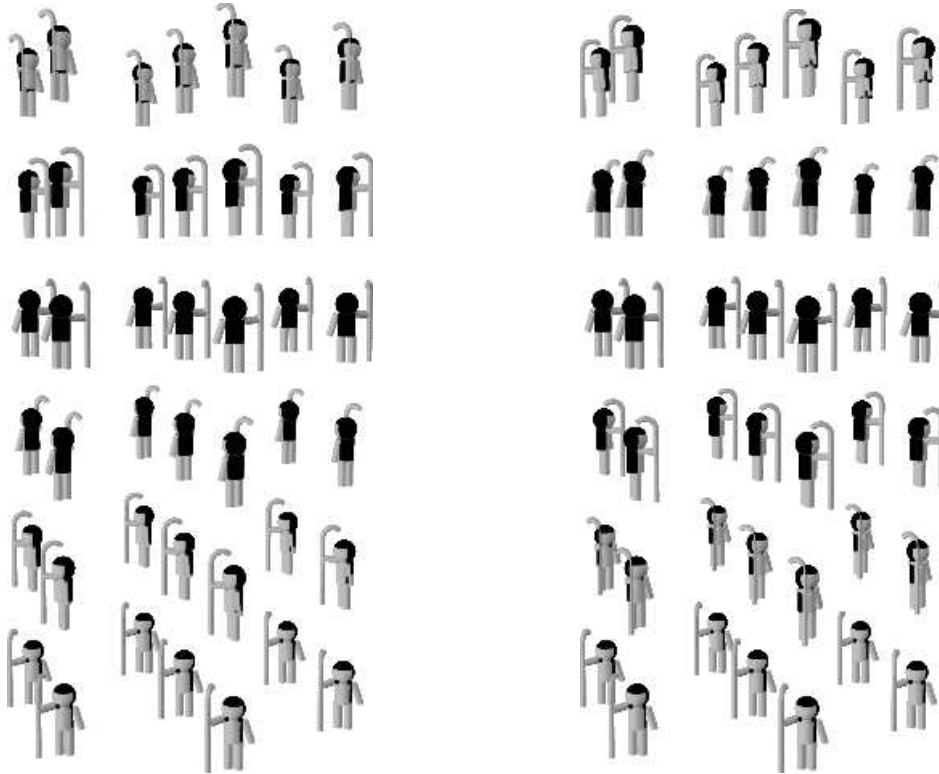


FIGURE 15. A sinistral hexacosm (left) and a dextral hexacosm (right).

The Didicosm $c22^{ABC}$. For the didicosm (see Figures 10 and 16), the naming lattice is generated by the three defining screw vectors $\mathbf{x}, \mathbf{y}, \mathbf{z}$, and so is a rectangular lattice Λ^{ABC} , whose conorms A, B, C are their squared lengths, say a^2, b^2, c^2 . The volume is $2abc$ (and so the *determinant*, or squared volume, is $4ABC$), since a fundamental region consists of two $a \times b \times c$ ‘boxes’, say the leading box labelled \mathbf{b} in Figure 10 and an adjacent one labelled \mathbf{o} .

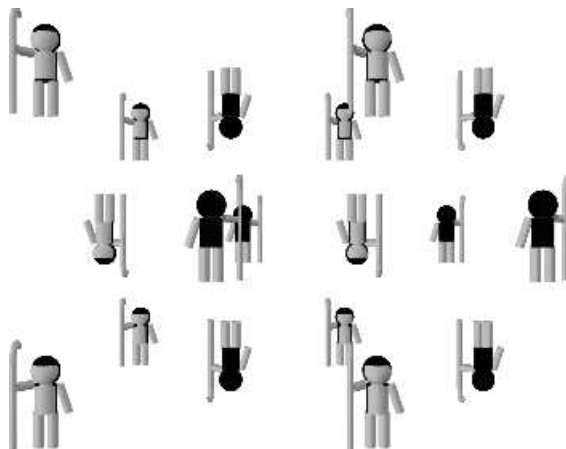


FIGURE 16. The dizziness of the didicosm! (Figure 10 may be more helpful.)

The Amphicosms $\pm a1_{A:BC}^D$. The naming lattice for the amphicosms $\pm a1_{A:BC}^D$ is the lattice $\mathcal{N} = \langle \mathbf{w}, \mathbf{x}, \mathbf{y}, \mathbf{z} \rangle$ (where $\mathbf{w} + \mathbf{x} + \mathbf{y} = 0$) with Gram-matrix

	\mathbf{w}	\mathbf{x}	\mathbf{y}	\mathbf{z}
\mathbf{w}	$A+B$	$-A$	$-B$	0
\mathbf{x}	$-A$	$A+C$	$-C$	0
\mathbf{y}	$-B$	$-C$	$B+C$	0
\mathbf{z}	0	0	0	D

, but we must point out the ‘anomaly’ that \mathbf{z}

plays different rôles in the two cases — it is a translation vector for $+a1$, but only half a translation vector for $-a1$: In consequence, the determinants are $D(AB + AC + BC)$ for $+a1$ and $4D(AB + AC + BC)$ for $-a1$. The translation lattices \mathcal{T} are $\langle 2\mathbf{x}, \mathbf{y}, \mathbf{z} \rangle$ and $\langle 2\mathbf{x}, 2\mathbf{y}, 2\mathbf{z}, \mathbf{y} + \mathbf{z} \rangle$, and $|\mathcal{N}/\mathcal{T}| = 2$ or 4 respectively (see Figure 17).

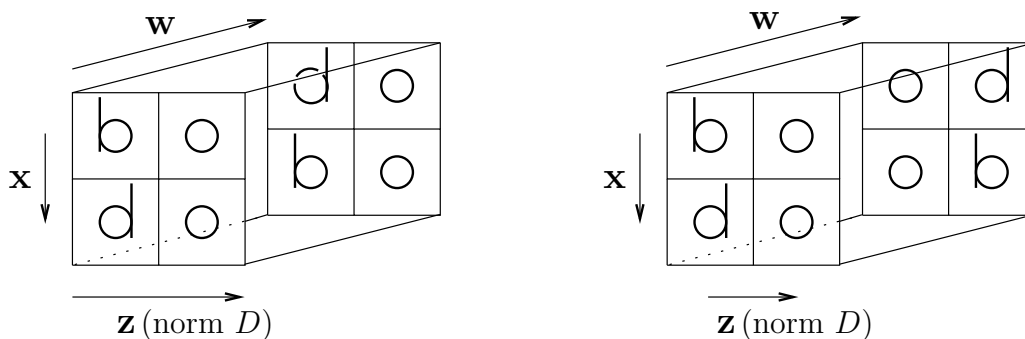


FIGURE 17. Defining vectors for the amphicosms.

The Amphidicosms $\pm a2_{A:B}^D$. For the amphidicosms the Gram-matrix

	x	y	z
x	A	0	0
y	0	B	0
z	0	0	D

shows that the Naming lattice $\mathcal{N} = \langle \mathbf{x}, \mathbf{y}, \mathbf{z} \rangle$ is a rectangular 3-dimensional lattice $\Lambda_{AB}^D \cong \Lambda^{ABD}$. We have the same anomaly about the meaning of \mathbf{z} , which leads to differing determinants: ABD for $+a1_{A:B}^D$ and $4ABD$ for $-a1_{A:B}^D$. The translation lattices \mathcal{T} are $\langle 2\mathbf{x}, 2\mathbf{y}, \mathbf{z} \rangle$ and $\langle 2\mathbf{x}, 2\mathbf{y}, 2\mathbf{z} \rangle$, and $|\mathcal{N}/\mathcal{T}| = 4$ or 8 respectively (see Figure 19).

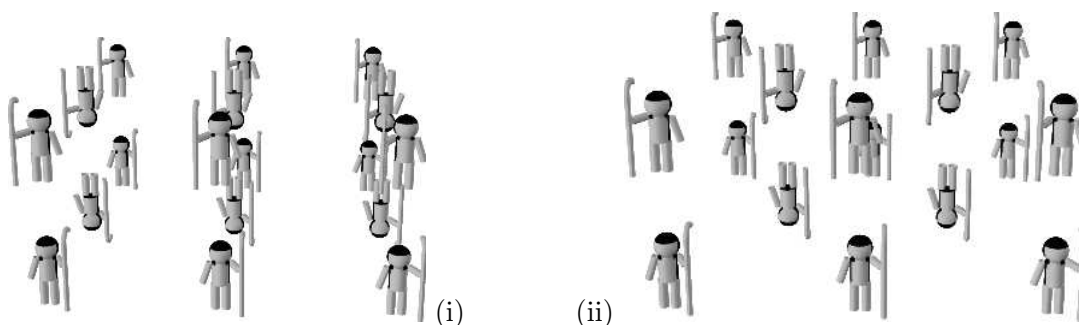


FIGURE 18. (i) a first amphidicosm $+a2$, and (ii) a second amphidicosm $-a2$.

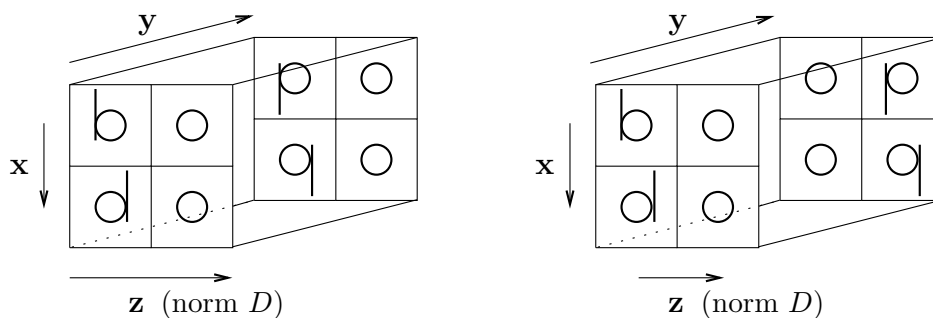


FIGURE 19. Defining vectors for the amphidicosms.

Which is which? It can be quite difficult to recognize which kind of amphicosm or amphidicosm one finds oneself in! Thus it took 20 years before it was noticed that the four figures of amphichiral platycosms in the celebrated book *The Shape of Space* [We1], only define two inequivalent manifolds!⁵

There are several ways to answer this question. One is that it is an *amphicosm* or *amphidicosm* according as its point group has size 2 or 4, and *first* or *second*

⁵Figures 7.7 and 7.10 in that book are two first amphicosms with different metrics, while Figures 7.11 and 7.12 are actually isometric first amphidicosms! To understand these equivalences, see the remark on ‘variant forms’ (2) in Section 3.

according as $|\mathcal{N}/\mathcal{T}|$ is 1 or 2 times this. However, the safest rule we have found is

An ‘amphi’ is of first or second type if and only if it has a glide mirror of first or second return, respectively.

The reflecting plane of a glide reflection (a *glide mirror*) is of *first* or *second return* if and only if the geodesic normal to its image at an arbitrary point closes exactly at its first or second return to the surface respectively.

So to find which kind of amphichiral platycosm you are in, starting from a general point of some glide mirror, walk perpendicularly to it until you first hit that mirror again. If this is always at the same point, you are in a first (or positive) ampicosm or amphidicosm — if always at a different point, in a second (or negative) one. But beware: in an amphidicosm, there are also ‘ambiguous’, glide mirrors that meet most normals twice, but some only once. For more details, see the next section.

5. EMBEDDED FLAT SURFACES

In this section, “embedded surface” always means “embedded compact flat 2-manifold”. It will be either a torus or a Klein bottle, and either type may be embedded either 1-sidedly or 2-sidedly⁶. Any such surface is the image of a plane in the universal cover with the property that modulo Γ it is compact.

Then the planes parallel to π will have the same properties and so yield other embedded surfaces. The configuration space of any such parallel family may be a circle, which we denote by $(2K)$ or $(2T)$ according as its elements (which are necessarily 2-sided) are Klein bottles or tori. Alternatively, it may be an interval, in which case only the extreme members will be 1-sided; we will write $[1K (2T) 1T]$ (say) for such an interval whose end surfaces are a 1-sided Klein bottle and a 1-sided torus, and whose interior surfaces are 2-sided tori.

It is useful to classify 1-sided surfaces more closely, which we do by inserting signs and the letters g and s . We write $+1$ for a first return (or ‘positive’) surface, meaning that the normal at any point p intersects it only at p , and -1 for a second return (or ‘negative’) one, when the normal at any p intersects it in exactly two distinct points (p and the ‘negative’ of p), and finally ∓ 1 for an ‘ambiguous’ one, which intersects most normals twice but some only once.

Again if a surface is 1-sided then there is either a glide reflection or a screw motion (or both) preserving it. We call it respectively a *glide surface* or *screw surface* (or both), and indicate this by the letters g or s (or gs). So $+1gT$ refers to a positive (1-sided) glide torus, $\mp 1sK$ to an ambiguous screw Klein bottle.

Since embedded flat 2-manifolds are the images of planes in the universal cover, we must look for such planes whose image modulo Γ is a torus or Klein bottle (the only compact possibilities).

⁶For surfaces embedded in Euclidean space, 2-sidedness is equivalent to orientability, but in more general 3-manifolds this is no longer true.

Some considerations limit the search. The plane π must not intersect any of its images under Γ other than itself, which entails that all its images are parallel. Equivalently, Γ preserves the family of parallel lines perpendicular to the plane.

There is a standard argument that usually proves π is *basal*, that is, parallel to $\langle \mathbf{x}, \mathbf{y} \rangle$, or *perpendicular*, that is, perpendicular to $\langle \mathbf{x}, \mathbf{y} \rangle$. For if not, a unit vector \mathbf{v} orthogonal to π would resolve into basal and perpendicular parts as $\mathbf{v} = \mathbf{v}_1 + \mathbf{v}_2$ with $\mathbf{v}_1 \neq \mathbf{0}, \mathbf{v}_2 \neq \mathbf{0}$. Since the typical operation $\gamma \in \Gamma$ takes this to $\mathbf{v} = \mathbf{v}'_1 + \mathbf{v}'_2$ where $\mathbf{v}'_2 = \pm \mathbf{v}_2$ we must have $\mathbf{v}'_1 = \pm \mathbf{v}_1$ with the same sign. However for every case other than *c1* we can find a γ for which this does not happen.

For the **hexacosm** *c6*, **tetracosm** *c4* and **tricosm** *c3* the argument actually proves more, for then the defining screw motion takes \mathbf{v}_1 to a vector \mathbf{v}'_1 which is not equal to $\pm \mathbf{v}_1$, unless $\mathbf{v}_1 = \mathbf{0}$, which forces $\mathbf{v} = \mathbf{v}_2$ and π to be basal. The basal planes yield a circular family ($2T$) of 2-sidedly embedded tori.

For the **dicosm** *c2* the same is true of the basal planes, but now there are also an infinite number of families of perpendicular planes, such as the family parallel to $\langle \mathbf{x}, \mathbf{z} \rangle$. These yield an interval [$1sK$ ($2T$) $1sK$] of embedded surfaces as suggested in Figure 20. We obtain a similar interval of perpendicular planes for each primitive vector \mathbf{x}' (counted up to sign) of the lattice $\langle \mathbf{x}, \mathbf{y} \rangle$, since any such vector appears in some basis \mathbf{x}', \mathbf{y}' . On the other hand, the standard argument shows that

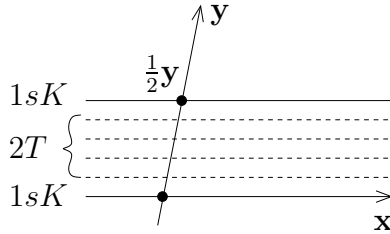


FIGURE 20. The extremes (through 0 and $\frac{1}{2}y$) are 1-sided Klein bottles while all others are 2-sided tori.

every embedded surface must be basal or perpendicular, since the defining screw motion takes \mathbf{v}_1 to $-\mathbf{v}_1$ but \mathbf{v}_2 to $+\mathbf{v}_2$. This shows that the infinity of intervals [$1sK$ ($2T$) $1sK$] of the preceding paragraph do indeed comprise all the non-basal embedded surfaces, agreeing with the entry $(2T)^1, [1sK$ ($2T$) $1sK]^\infty$ in Table 4.

For the **torocosm** *c1* the standard argument does not apply, but the answer is easy — there is a circular family ($2T$) of 2-sided tori corresponding to each 2-dimensional section⁷ of $\mathcal{T} = \langle \mathbf{x}, \mathbf{y}, \mathbf{z} \rangle$, or equivalently to each pair of primitive vectors $\pm \mathbf{v}^*$ of the dual lattice \mathcal{T}^* , yielding the entry $(2T)^\infty$ in Table 4.

For the **didicosm** *c22* the standard argument can be applied in different directions, showing that π must be parallel or perpendicular to $\langle \mathbf{y}, \mathbf{z} \rangle$ as well as to $\langle \mathbf{x}, \mathbf{y} \rangle$, which forces it to be parallel to one of the three coordinate planes $\langle \mathbf{x}, \mathbf{y} \rangle, \langle \mathbf{x}, \mathbf{z} \rangle, \langle \mathbf{y}, \mathbf{z} \rangle$. We obtain three intervals of type $[\mp 1sK$ ($2T$) $\mp 1sK]$ (Figure 21).

⁷a section of a lattice is its full intersection with some subspace.

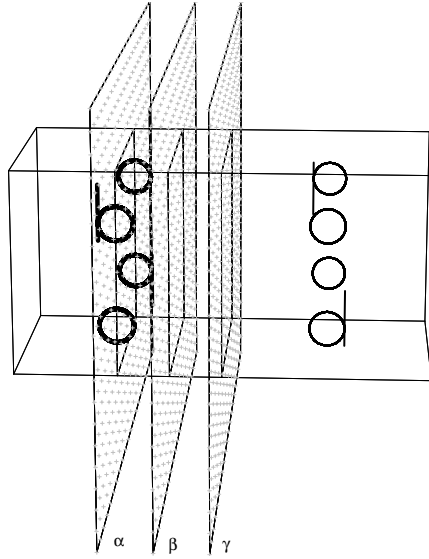


FIGURE 21. The plane α is a Klein bottle, which is embedded 1-sidedly as shown by the screw motion taking \mathbf{b} to \mathbf{q} , and the same is true for γ as shown by that taking \mathbf{b} to \mathbf{d} . In view of these two screw motions, we need only consider planes like β between α and γ — these are 2-sided tori.

For the **amphicosms** $\pm a1$ the standard argument applies since the glide reflection takes \mathbf{v}_1 to $+\mathbf{v}_1$ but \mathbf{v}_2 to $-\mathbf{v}_2$. We first handle the perpandal planes.

We can see that the planes parallel to $\langle \mathbf{x}, \mathbf{z} \rangle$ or $\langle \mathbf{y}, \mathbf{z} \rangle$ yield circles of 2-sided Klein bottles and 2-sided tori respectively, since \mathbf{x} is a glide vector and \mathbf{y} is a translation vector.⁸ But any primitive vector of $\langle \mathbf{x}, \mathbf{y} \rangle$ belongs to a superbase $\mathbf{w}', \mathbf{x}', \mathbf{y}'$ whose vectors are respectively congruent modulo 2 to $\mathbf{w}, \mathbf{x}, \mathbf{y}$, which makes \mathbf{w}', \mathbf{x}' be glide vectors and \mathbf{y}' a translation vector, and any such superbase is equivalent to $\mathbf{w}, \mathbf{x}, \mathbf{y}$ by some isotopy of the lattice. So the perpandal planes yield infinitely many circles of each type $(2K)$ or $(2T)$. The basal planes form an interval of type $[+1gT (2T) +1gT]$ for $+a1$, $[-1gT (2T) -1gT]$ for $-a1$.

Finally, for the **amphidicosms** $\pm a2$ the standard argument applies in both $\langle \mathbf{x}, \mathbf{y} \rangle$ and $\langle \mathbf{x}, \mathbf{z} \rangle$ directions, showing that π must be parallel to a coordinate plane. The perpandal planes parallel to $\langle \mathbf{x}, \mathbf{z} \rangle$ form a circle $(2K)$ and those parallel to $\langle \mathbf{y}, \mathbf{z} \rangle$ an interval $[\mp 1sK (2T) \mp 1gK]$ while the basal planes (parallel to $\langle \mathbf{x}, \mathbf{y} \rangle$) form an interval of type $[+1gsK (2K) +1gsK]$ for $+a2$ and $[-1gT (2T) -1sK]$ for $-a2$.

We summarize the results in Table 4.

⁸In view of the symmetry interchanging \mathbf{w} and \mathbf{x} , the planes parallel to $\langle \mathbf{w}, \mathbf{z} \rangle$ behave like those parallel to $\langle \mathbf{x}, \mathbf{z} \rangle$.

platycosm	families of surfaces	
c1		$(2T)^\infty$
c2	$(2T)^1$;	$[1sK (2T) 1sK]^\infty$
c3		$(2T)^1$
c4		$(2T)^1$
c6		$(2T)^1$
c22		$[\mp 1sK (2T) \mp 1sK]^3$
+a1	$[+1gT (2T) +1gT]^1$;	$(2K)^\infty, (2T)^\infty$
-a1	$[-1gT (2T) -1gT]^1$;	$(2K)^\infty, (2T)^\infty$
+a2	$[+1gsK (2K) +1gsK]^1$;	$(2K)^1, [\mp 1sK (2T) \mp 1gT]^1$
-a2	$[-1gT (2T) -1sK]^1$;	$(2K)^1, [\mp 1sK (2T) \mp 1gT]^1$

TABLE 4. The parallel families of embedded surfaces, with the type symbol defined in the text and the number of families of this type indicated by the superscript. Those before a semicolon are images of basal planes, those after of perpendal ones.

6. INFINITE PLATYCOSMS

Although elsewhere in this paper ‘platycosm’ means ‘finite platycosm’, in this section we briefly discuss and name the infinite ones. An *infinite platycosm* is a boundaryless flat manifold that has infinite volume, or equivalently is not compact.

One kind of infinite platycosm, the ‘Product Space’ or *Prospace*, is topologically the cartesian product of a compact flat manifold of dimension 0, 1, 2 by a Euclidean space of the complementary dimension 3, 2, 1. The cases are

compact factor	complementing (fiber) space	name	notation and parameters
Point	\mathbb{R}^3	Euclidean Space	EUC
Circle	\mathbb{R}^2	Circular Prospace	$CPS_A(\theta)$
Torus	\mathbb{R}^1	Toroidal Prospace	TPS_{ABC}
Klein Bottle	\mathbb{R}^1	Kleinian Prospace	KPS_B^A

The others are related to these in the way a Möbius strip is to an annulus, so we call them *Möbius spaces*, or ‘Mospaces’. Technically, they are fibrations whose base is a compact flat submanifold of dimension 1 or 2 and whose fiber is the ‘complementary’ Euclidean space of dimension 2 or 1, which is reflected when we traverse at least one closed path in the base. This path must be homotopically non-trivial and may be orientation preserving (+) or orientation-reversing (-). The cases are

compact base	compl. fiber	path type	name	notation and parameters
Circle	\mathbb{R}^2	+	Circular Mospace	CMS_A
Torus	\mathbb{R}^1	+	Toroidal Mospace	$TMS_{A:B:C}$
Klein Bottle	\mathbb{R}^1	-	chiral Kleinian Mospace	$+KMS_B^A$
Klein Bottle	\mathbb{R}^1	+	achiral Kleinian Mospace	$-KMS_B^A$

Figures 22, 23 and 24 picture these manifolds (strictly, their universal covers). The group for $CPS_A(\theta)$ is generated by a screw motion of angle θ and length \sqrt{A} . In the *untwisted* case when $\theta = 0$ this is the direct product of a circle and a plane even in the metrical sense, in the twisted cases (when θ is not a multiple of 2π) it is only topologically so.

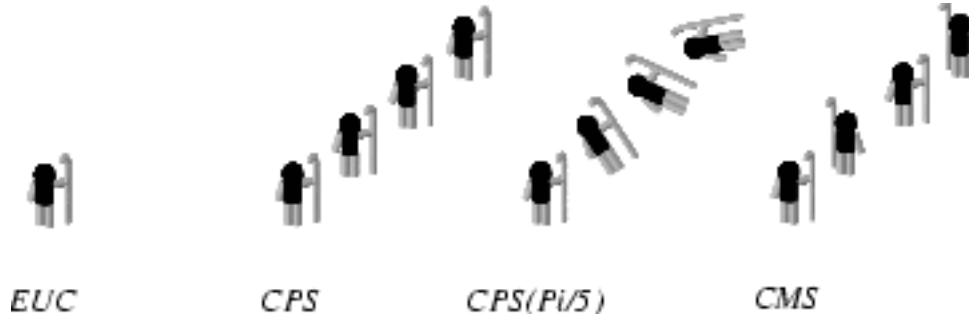


FIGURE 22. One's images in the simplest infinite platycosms.

In $CPS_A(\theta) (= CPS_{\boxed{a}}(\theta))$ there is always a closed geodesic of length $a = \sqrt{A}$: this is the only primitive closed geodesic unless $\frac{\theta}{2\pi}$ is rational, when the associated screw motion has a finite period N , and all geodesics parallel to it are closed, of length aN . For $CMS_A (= CMS_{\boxed{a}})$ the group is generated by a glide reflection of length $a = \sqrt{A}$. The manifolds described so far are illustrated in Figure 22.

For TPS_{ABC} the group is a 2-dimensional lattice of translations for which some superbasis $\mathbf{v}_0, \mathbf{v}_1, \mathbf{v}_2$ has conorms A, B, C . In $TMS_{A:B:C}$ the translations through \mathbf{v}_0 and \mathbf{v}_1 (so *not* \mathbf{v}_2) are replaced by the glide reflections obtained by combining them with the reflection in the base plane $\langle \mathbf{v}_0, \mathbf{v}_1, \mathbf{v}_2 \rangle$. These manifolds appear in Figure 23.

The group for $KPS_B^A (= KPS_{\boxed{\frac{a}{b}}})$ is generated by a translation along \mathbf{v}_1 of length $a = \sqrt{A}$ and a glide reflection along a vector \mathbf{v}_2 of length $b = \sqrt{B}$ perpendicular to \mathbf{v}_1 whose reflecting plane is orthogonal to the base plane $\langle \mathbf{v}_1, \mathbf{v}_2 \rangle$. For $+KMS_B^A (= +KMS_{\boxed{\frac{a}{b}}})$ we compose the latter with the reflection in the base plane, so that it becomes a screw motion. For $-KMS_B^A (= -KMS_{\boxed{\frac{a}{b}}})$ we instead compose the former with that reflection, so making it a glide reflection. Figure 24 shows these three Kleinian manifolds.

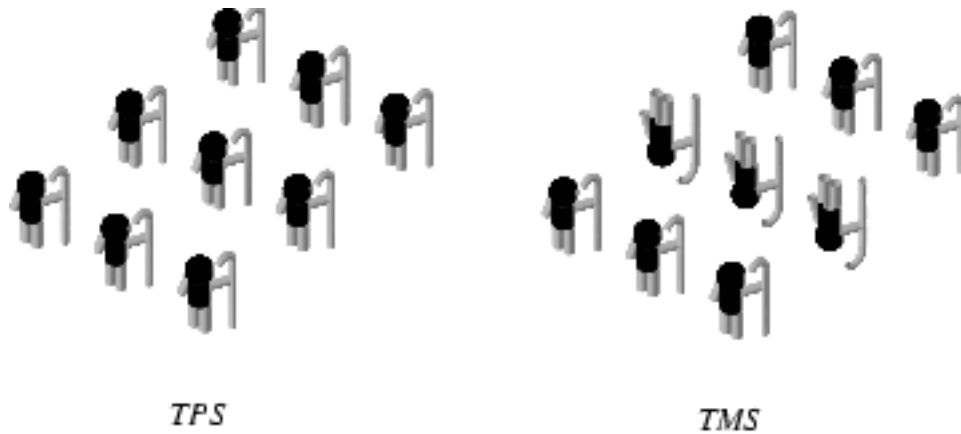


FIGURE 23. The toroidal Product and Möbius spaces.



FIGURE 24. Kleinian Product and Möbius spaces.

Beware: not every 3-dimensional product of flat manifolds is a ‘Prospace’ — we use that term only for the product of a compact manifold and a Euclidean space. The following little table shows that no fewer than 8 of the 18 platycosm types include non-trivial direct products (Table 5).

product of	line	circle
plane	<i>EUC</i>	<i>CPS</i> *
cylinder	<i>CPS</i> *	<i>TPS</i> *
Möbius cylinder	<i>CMS</i>	<i>TMS</i> *
torus	<i>TPS</i>	<i>c1</i> *
Klein bottle	<i>KPS</i>	<i>+a1</i> *

TABLE 5. An asterisk indicates that the metrical direct products of this kind do not yield all parameter sets in this case.

7. FUNDAMENTAL GROUPS, HOMOLOGY AND AUTOMORPHISMS

The fundamental group of a platycosm is just the space group Γ we see in its universal cover. We explain how to find a presentation, using the amphisoms and amphidicosms as our examples. Let us mark any letter \mathbf{b} , \mathbf{d} , \mathbf{p} , \mathbf{q} in our diagrams with the element of Γ by which it can be obtained from the initial \mathbf{b} — this sets up a 1-1 correspondence, since these letters have no symmetry.⁹ Then a presentation for Γ can be computed as follows. First find generators for Γ , and then generators for \mathcal{T} in terms of these. Then a set of relations will be sufficient if and only if they imply the correct structures for

- i) the subgroup \mathcal{T} ;
- ii) the action of each generator on \mathcal{T} ;
- iii) the point group $G = \Gamma/\mathcal{T}$.

Since the two amphisoms $\pm a1$ are the hardest cases, we discuss them in detail. It is easy to see that the operations W, X, Z defined by Figures 17 and 25 are generators. The vectors associated to these are \mathbf{w}, \mathbf{x} and $\mathbf{z}' = \mathbf{z}$ or $2\mathbf{z}$, and we see that the translation lattice is generated in each case by $2\mathbf{w}, 2\mathbf{x}, \mathbf{w} + \mathbf{x}, \mathbf{z}'$, showing that the subgroup \mathcal{T} is generated by W^2, X^2, WX, Z .

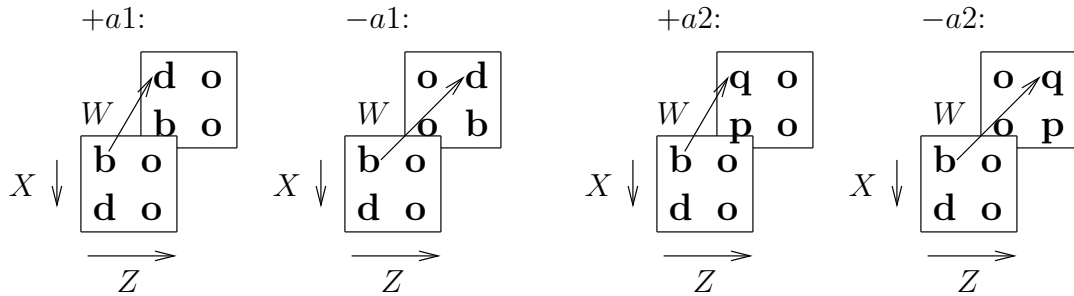


FIGURE 25. Generators for the ‘amphis’. In these, X is always a glide reflection with vector \mathbf{x} that takes the leading \mathbf{b} to the \mathbf{d} below it, while Z is the translation with vector \mathbf{z} or $2\mathbf{z}$ that takes it to the next \mathbf{b} to its right. For $+a1$, W is a glide reflection with vector \mathbf{w} . For $-a1$, it is a glide reflection with vector $\mathbf{w} + \mathbf{z}$ while the W ’s for $\pm a2$ are (different) screw motions, with vectors \mathbf{y} .

We obtain the correct structure for \mathcal{T} by demanding that these commute, and that $(WX)^2 = W^2X^2$ or W^2X^2Z in the two cases. Let us suppose in general that we have found some generators G_1, G_2, \dots for Γ , and certain products w_1, w_2, \dots of them that generate \mathcal{T} , and relations R_1, R_2, \dots that define its structure. Our next step is to define the correct action on \mathcal{T} , for which it suffices to express each $w_i^{G_j} = G_j^{-1}w_iG_j$ as a function of the w_i . For the first amphicosm, we find that W^2 and X^2 are fixed by all three of W, X, Z , while Z is fixed by itself (obviously), but inverted by each of W and X , so we add these assertions as relations.

⁹Not even front-to-back!

Finally, we must ensure that our relations imply the correct structure for the point group $G = \Gamma/\mathcal{T}$. However, for the amphicosms they already do, since modulo \mathcal{T} we have $W^2 \equiv X^2 \equiv WX \equiv Z \equiv 1$, which show that in the point group, W and X map to the same element of order two, while Z maps to 1.

The relations one obtains in this way can almost always be simplified. The best way to do this is to adjoin the shortest relations one can find and then delete any redundant ones. For the first or second amphicosms, we find three simple relations, namely

$$Z^W = Z^X = Z^{-1} \quad \text{and} \quad W^X = W \text{ or } ZW$$

in the two cases.

The fact that W, X invert Z implies that W^2, X^2, WX commute with Z . But also, these three relations imply that W^2 commutes with X^2 — obviously for the first amphicosm, while for the negative one $ZW^2Z^W = ZW^2Z^{-1} = W^2$. Moreover, they imply that

$$XWXW = X^2W^XW = X^2(1 \text{ or } Z)W^2,$$

which was the further relation needed for the structure of \mathcal{T} .

Finally, our three simple relations specify the action of W, X on Z and each other, so in particular on W^2, X^2, WX, Z , the generators of \mathcal{T} . Rewriting the last relation as

$$[X, W] = 1 \text{ or } Z,$$

we see that:

The fundamental groups of the amphicosms have presentations:

$$\begin{aligned} \text{for } +a1 \quad & \langle W, X, Z : Z^X = Z^W = Z^{-1}, [X, W] = 1 \rangle \\ \text{for } -a1 \quad & \langle W, X, Z : Z^X = Z^W = Z^{-1}, [X, W] = Z \rangle. \end{aligned}$$

Of course, their first homology groups are obtained by abelianizing these. They are

$$\begin{aligned} \text{for } +a1 \quad & \langle W, X, Z \mid \text{abelian}, Z^2 = 1 \rangle \cong C_2 \times C_\infty \times C_\infty \\ \text{for } -a1 \quad & \langle W, X, Z \mid \text{abelian}, Z = 1 \rangle \cong C_\infty \times C_\infty, \end{aligned}$$

since in the $+a1$ case Z was conjugate to Z^{-1} , so Z^2 maps to 1, while for $-a1$ Z was a commutator, so itself maps to 1. In Table 6, we abbreviate these group structures to $2 \cdot \infty^2$ and ∞^2 .

Helicosms. For the helicosms we have the presentations of the table, in which Z is the defining screw motion, while X and Y generate the 2-dimensional lattice perpendicular to it.

Didicosm. For the didicosm $c22$ we find in this way that the translation subgroup is generated by the squares of the generating screw motions X, Y, Z , which invert the squares of each other, and satisfy $XYZ = 1$. It turns out that this presentation reduces to $\langle X, Y \mid X = Y^2XY^2, Y = X^2YX^2 \rangle$ when we define $Z = (XY)^{-1}$. The abelianization is $C_4 \times C_4$, which we denote by 4^2 . This proves the well known fact that the Hantzsche-Wendt didicosm $c22$ is the only platycosm with finite homology, or equivalently, with zero first Betti number.

	presentation	H_1	transl. lattice
$c1$	$X \rightleftharpoons Y \rightleftharpoons Z \rightleftharpoons X$	∞^3	X, Y, Z
$c2$	$X \rightleftharpoons Y$ $Z : X \rightarrow X^{-1}, Y \rightarrow Y^{-1}$	$2^2 \cdot \infty$	X, Y, Z^2
$c3$	$X \rightleftharpoons Y$ $Z : X \rightarrow Y \rightarrow (XY)^{-1}$	$3 \cdot \infty$	X, Y, Z^3
$c4$	$X \rightleftharpoons Y$ $Z : X \rightarrow Y \rightarrow X^{-1}$	$2 \cdot \infty$	X, Y, Z^4
$c6$	$X \rightleftharpoons Y$ $Z : X \rightarrow XY \rightarrow Y$	∞	X, Y, Z^6
$c22$	$\langle X, Y X = Y^2XY^2, Y = X^2YX^2 \rangle$	4^2	$X^2, Y^2, Z^2 = (XY)^{-2}$
$+a1$	$W, X : Z \rightarrow Z^{-1}, [X, W] = 1$	$2 \cdot \infty^2$	W^2, X^2, WX, Z
$-a1$	$W, X : Z \rightarrow Z^{-1}, [X, W] = Z$	∞^2	W^2, X^2, WX, Z
$+a2$	$W, X : Z \rightarrow Z^{-1}, W : X \rightarrow X^{-1}$	$2^2 \cdot \infty$	W^2, X^2, Z
$-a2$	$W, X : Z \rightarrow Z^{-1}, W : X \rightarrow X^{-1}Z$	$4 \cdot \infty$	W^2, X^2, Z

TABLE 6.

We remark that the fundamental groups of $c1, c2, +a1, +a2$ need three generators; each of the others can be generated by two elements.

Automorphisms. The largest group of ‘symmetries’ of Γ is its *affine normalizer*¹⁰, which consists of the affine automorphisms of \mathbb{R}^3 that take Γ into itself. We discuss the four ‘parts’ of this group¹¹ illustrated in Fig. 26:

Part I is the *connected part* (the component of the identity), which by continuity must fix Γ pointwise since the identity does. In other words, it is central. For the platycosms, it consists only of translations and its dimension is the first Betti number β_1 . It is a subtle theorem (cf. [ChV]) that factoring out part I yields precisely the automorphisms of Γ .¹²

Part II, the *inner part*, is the space group Γ , which acts trivially on M , but (of course) induces inner automorphisms on Γ . Since these induce the identity on M , they must be factored out to obtain the group of affinities of M .

The intersection of parts I and II is the translation subgroup of Γ . If we factor out both, we obtain the outer automorphism group of Γ , which is equally

¹⁰so called because it is the normalizer of Γ in the group of affine transformations of \mathbb{R}^3 .

¹¹Beware: these ‘parts’ are not always subgroups and not always disjoint.

¹²Our argument, although it refers to the way an automorphism acts on Γ , does not in fact use this theorem.

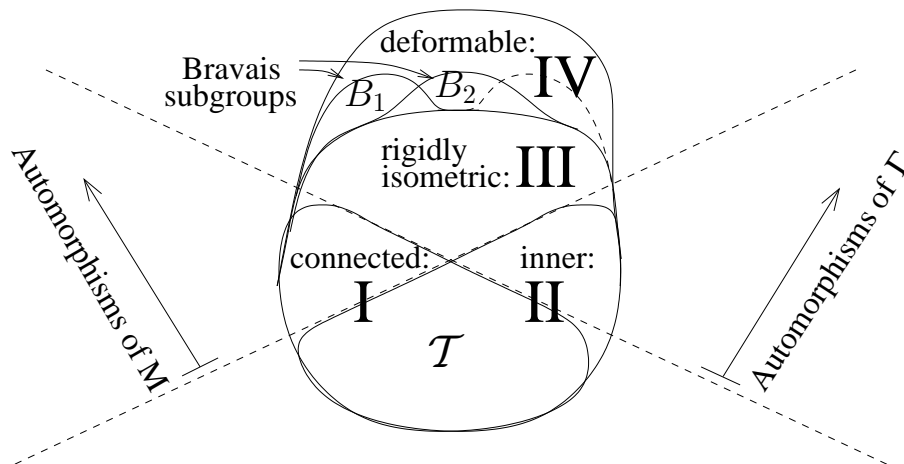


FIGURE 26.

the discontinuous part of the (affine) symmetry-group of M . The elements of the connected and inner parts are isometric, but not all elements of the outer automorphism group need be so. We therefore separate it into:

Part III, the *rigidly isometric part*, the normal subgroup that contains precisely those elements that are isometric for all the values of the parameters. Factoring these out, we obtain:

Part IV, the *deformable part*. For example, the variant form (2) for $+a1$ shows that it has an automorphism interchanging W and X (see Fig. 17), which is not always an isometry. It will however become an isometry if $B = C$. In general there are certain finite subgroups, the *Bravais subgroups* B_1, B_2, \dots , of the deformable part that just consist of the symmetries that can become isometric for various choices of the parameters. They are completely enumerated in Section 11.

Combining the results of that section and this, our paper describes all isometries of all platycosms.

These groups are tabulated in Table 7. We shall discuss only the two hardest cases, $c22$ and $-a1$.

The second amphi-cosm. For $-a1$ it is easily checked that the most general inner automorphism (m, n, σ) , say, takes $W \rightarrow WZ^m, X \rightarrow XZ^n, Z \rightarrow Z^\sigma$, where $\sigma = \pm 1, m - n = \frac{\sigma-1}{2}$, the ones induced by W, X, Z being $(0, +1, -), (-1, 0, -), (2, 2, +)$, respectively.

Now the glide planes of $-a1$ form a parallel series, say

$$\dots \left| \begin{array}{c} \pi_{-1} \\ \vdots \end{array} \right| \left| \begin{array}{c} \pi_0 \\ \vdots \end{array} \right| \left| \begin{array}{c} \pi_1 \\ \vdots \end{array} \right| \left| \begin{array}{c} \pi_2 \\ \vdots \end{array} \right| \dots \left| \dots \right| \dots$$

and the inner automorphisms can move the W and X planes (say π_0 and π_1) any even number of steps, while the further automorphism that takes (W, X, Y) to (WZ, XZ, Z^{-1}) moves them just one step.

Modulo these we may suppose π_0 and π_1 are fixed or interchanged. The most general automorphism that does this is

$$W \rightarrow W^a X^b, \quad X \rightarrow W^c X^d, \quad Z \rightarrow Z^\epsilon \quad (\epsilon = \pm 1),$$

where

$$(4) \quad \text{if } \epsilon = +1, \quad \begin{bmatrix} a & b \\ c & d \end{bmatrix} \equiv \begin{bmatrix} 1 & 0 \\ 0 & 1 \end{bmatrix} \pmod{2}, \quad \text{while}$$

$$(5) \quad \text{if } \epsilon = -1, \quad \begin{bmatrix} a & b \\ c & d \end{bmatrix} \equiv \begin{bmatrix} 0 & 1 \\ 1 & 0 \end{bmatrix} \pmod{2}.$$

The group defined by (4) is often called $\Gamma(2)$. This explains the entry in Table 7.

The Didicosm. To fix our ideas we take $A = B = C = 1$. Then the generators X, Y are two screw motions of the minimal length 1 at the minimal distance $1/2$. The same must be true of their images, since if either length or distance were to be increased the resulting elements would no longer generate. Now X, Y determine Z via $XYZ = 1$. The lines of these three generators are edges of a unique $\frac{1}{2} \times \frac{1}{2} \times \frac{1}{2}$ cube (or ‘cubelet’) that constitutes one eighth of our defining ‘box’. The general automorphism will take it to a similar cubelet, constituting an eighth of some other box of the tessellation.

We first show that there are enough automorphisms to take this standard cubelet to any of the eight cubelets in any box. It may be taken to the corresponding one in any other box by a translation through a typical vector $\alpha \mathbf{x} + \beta \mathbf{y} + \gamma \mathbf{z}$ of the naming lattice $\mathcal{N} = \langle \mathbf{x}, \mathbf{y}, \mathbf{z} \rangle$, which achieves

$$(X, Y, Z) \mapsto (XY^{2\beta} Z^{2\gamma}, YX^{2\alpha} Z^{2\gamma}, ZX^{2\alpha} Y^{2\beta}).$$

(This is inner just if α, β, γ are even, since then the associated translation belongs to $\mathcal{T} = \langle 2\mathbf{x}, 2\mathbf{y}, 2\mathbf{z} \rangle$.)

The automorphisms we have just found effectively allow us to suppose that there is only one box, which contains just eight cubelets. The inner automorphisms by X, Y, Z take the standard cubelet to four of these. (We have now found all inner automorphisms, since these elements represent the four cosets of \mathcal{T} in Γ .)

So we need only find a further automorphism that takes the standard cubelet to one of the missing four. This is

$$(X, Y, Z) \mapsto (YZ^{-1}, ZX^{-1}, XY^{-1}).$$

(the latter three elements are half turn screw motions about lines bisecting the other three faces of the standard box.)

All the above automorphisms fix the three coordinate directions, so will be isometric even in the general case (A, B, C distinct). Modulo them, we can suppose X, Y, Z go to some permutation of $X^{\pm 1}, Y^{\pm 1}, Z^{\pm 1}$, since these are the only length 1 screw motions associated with the initial cubelet. The condition $XYZ = 1$ restricts us to the cyclic permutations of X, Y, Z or Z^{-1}, Y^{-1}, X^{-1} . The identity is the only one of these that is isometric in the general case.

	I	II	III	IV	V	
	β_1	inner automorphisms	outer automorphisms		# of B_i 's	
			rigidly isometric	deformable		
c1	3	trivial	X^{-1}, Y^{-1}, Z^{-1}	2	$PGL_3(\mathbb{Z})$ on X, Y, Z	14
c2	1	$X^\epsilon, Y^\epsilon, X^a Y^b Z$: $a, b \in 2\mathbb{Z}$	X, Y, XZ X, Y, YZ X, Y, Z^{-1}	2^3	$PGL_2(\mathbb{Z})$ on X, Y	5
c3	1	$X, Y, X^a Y^b Z$ $Y, W, X^a Y^b Z$ $W, X, X^a Y^b Z$: $a + b \in 3\mathbb{Z}$	X, Y, XZ X^{-1}, Y^{-1}, Z Y, X, Z^{-1}	$2 \times S_3$	1	1
c4	1	$X, Y, X^a Y^b Z$ $Y, X^{-1}, X^a Y^b Z$ $X^{-1}, Y^{-1}, X^a Y^b Z$ $Y^{-1}, X, X^a Y^b Z$: $a + b \in 2\mathbb{Z}$	X, Y, XZ Y, X, Z^{-1}	2^2	1	1
c6	1	$X^\sigma, Y^\sigma, X^a Y^b Z$ $Y^\sigma, W^\sigma, X^a Y^b Z$ $W^\sigma, X^\sigma, X^a Y^b Z$: $\sigma = \pm 1, a + b \in \mathbb{Z}$	Y, X, Z^{-1}	2	1	1
c22	0	$X^T Y^b Z^c, Y^T X^a Z^c, Z^T X^a Y^b$: $a, b, c \in 4\mathbb{Z}, T = 1, X, Y, Z$	$X, Y X^2, Z X^2$ $X Y^2, Y, Z Y^2$ $X Z^2, Y Z^2, Z$ $Y Z^{-1}, Z X^{-1}, X Y^{-1}$	2^4	S_3	3
+a1	2	$W Z^m, X Z^m, Z^\sigma$: $\sigma = \pm 1, m \in 2\mathbb{Z}$	$W Z, X Z, Z^{-1}$	2	$\Gamma(2)$ on W, X X, W, Z^{-1}	5
-a1	2	$W Z^m, X Z^n, Z^\sigma$: $\sigma = \pm 1, m - n = \frac{\sigma-1}{2}$	$W Z, X Z, Z^{-1}$	2	$\Gamma(2)$ on W, X X, W, Z^{-1}	5
+a2	1	$W X^{2a} Z^{2b}, X^\delta Z^{2b}, Z^\epsilon$: $\delta, \epsilon = \pm 1, 2a \equiv \delta - \epsilon \pmod{4}$	$W Z, X Z, Z$ W^{-1}, X, Z W, X^{-1}, Z	2^3	1	1
-a2	1	$W X^a Z^b, X^\delta Z^c, Z^\epsilon$: $\delta, \epsilon = \pm 1, 2c + \delta \equiv 1 \pmod{4}$ $a \equiv \delta - \epsilon \pmod{4}, 2b + 1 = 2c + \epsilon$	$W Z, X Z, Z$ W^{-1}, X, Z W, X^{-1}, Z	2^3	1	1

TABLE 7. Columns I–IV concern the appropriate parts. Thus I gives the dimension of the connected component, II the generic inner automorphisms, III generators and structure (modulo inner automorphisms) of the rigidly isometric part, IV the deformable part. Column V gives the number of distinct types of Bravais subgroups B_i (see Section 11). Automorphisms are specified by giving images of X, Y, Z for the chiral platycosms, W, X, Z for the achiral ones.

The conclusion is that the general inner automorphism takes (X, Y, Z) to

$$(X^T Y^{2\beta} Z^{2\gamma}, Y^T X^{2\alpha} Z^{2\gamma}, Z^T X^{2\alpha} Y^{2\beta}), \quad (\alpha, \beta, \gamma \text{ even}, T = 1, X, Y, Z);$$

while the full automorphism group is obtained by letting α, β, γ be arbitrary integers, and adjoining the maps taking (X, Y, Z) to any even permutation of (X, Y, Z) or $(YZ^{-1}, ZX^{-1}, XY^{-1})$ or any odd permutation of the inverses of those. Note that the argument proves $c22^{ABC}$ to be invariant under all permutations of A, B, C (not just the more obvious even ones).

Let $\theta_1, \theta_2, \theta_3, \phi$ be the automorphisms that take (X, Y, Z) to

$$(X, YX^2, ZX^2), (XY^2, Y, ZY^2), (XZ^2, YZ^2, Z), (YZ^{-1}, ZX^{-1}, XY^{-1}).$$

Then it is easily checked that modulo inner automorphisms, $\theta_1, \theta_2, \theta_3, \phi$ are multiplicatively commuting elements of order two. The elements π that take (X, Y, Z) to even permutations of (X, Y, Z) or odd permutations of (X^{-1}, Y^{-1}, Z^{-1}) form an S_3 that acts in the obvious way on $\theta_1, \theta_2, \theta_3$ and takes ϕ to itself or $\theta_1\theta_2\theta_3\phi$, according as π is even or odd. This shows that the outer automorphism group is a split extension $2^4:S_3$. The structure of this group was found (in a different form) by Zimmermann [Zi], who disproved an earlier assertion ([ChV], [Ch]) that the group was a split extension of form $2^3:(2 \times S_3)$.

The outer automorphism groups of flat manifolds have often been studied (e.g., [Ch], [MS], [Hi]), the last of which used them to enumerate compact flat 4-manifolds. Our treatment avoids uses of subtle theorems, and clearly distinguishes the isometric part.

8. DOUBLE COVERS

A double cover of a manifold M determines and is determined by a homomorphism from its fundamental group $\pi_1(M)$ onto $\{\pm 1\}$, the image of a path being -1 just if it interchanges the two sheets. To enumerate such homomorphisms, we can obviously abelianize $\pi_1(M)$ (to $H_1(M)$) and then make $H_1(M)$ have exponent 2, turning it into an elementary abelian 2-group. If there are r generators after this, the number of double covers will be $2^r - 1$. We discuss the cases.

Torocosm. Since $H_1(M) = \infty^3$, a torocosm has 7 double covers, themselves all torocosms.

Dicosm. Now $H_1(M) = 2^2 \cdot \infty$, so the dicosm also has 7 double covers, of which just one is a torocosm. Each of the other 6 is a dicosm, since some period 2 screw motion survives in the kernel of its defining homomorphism.

Tricosm. Since W, X, Y are conjugate in $\pi_1(M)$, they must map to the same sign, which must be $+$, since $WXY = 1$. There is therefore just one double cover (given by $W \mapsto +, X \mapsto +, Y \mapsto +, Z \mapsto -$) which is another tricosm $c3$.

Hexacosm. A similar argument shows that the hexacosm $c6$ also has a single double cover, a tricosm $c3$.

Tetracosm. X and Y are again conjugate, but now can both map to $+$ or both to $-$. There are therefore three double covers: $(X, Y, Z) \mapsto + + -$ (type $c2$) or $- - +$ or $- - -$ (both of type $c4$).

Didicosm. The relation $XYZ = 1$ shows that two of X, Y, Z must map to $-$ and the third to $+$. So we have three double covers, all dicosms $c2$.

Amphicosms and Amphidicosms. The abelianized groups show that the positive cases each have seven double covers and the negative ones three. The types are

- for $+a1$: 1 of type $c1$, 4 of type $+a1$, 2 of type $-a1$;
- for $-a1$: 1 of type $c1$, 2 of type $+a1$;
- for $+a2$: 1 of type $c2$, 2 of type $+a1$, 2 of type $+a2$, 2 of type $-a2$;
- for $-a2$: 1 of type $c2$, 2 of type $+a1$.

platycosm	generators $W X Y Z$	double covering	#	total #
$c1$		$c1$	7	7
$c2_{ABC}^D$	$(+++)-$ $(+--)\pm$	$c1_{ABC}^{4D}$ $c2_{[A]BC}^D$, etc.	1 2 of each	7
$c3_{AAA}^D$	$(+++)-$	$c3_{AAA}^{4D}$	1	1
$c4_{AA}^D$	$(++)-$ $(--)\pm$	$c2_{AA}^{4D}$ $c4_{2A2A}^D$	1 1 of each	3
$c6_{AAA}^D$	$(+++)-$	$c3_{AAA}^{4D}$	1	1
$c22^{ABC}$	$(+--)$	$c2_{4B4C}^A$, etc.	1 of each	3

X	Y	Z	$+a1_{A:BC}^D$	$-a1_{A:BC}^D$	$+a2_{A:B}^D$	$-a2_{A:B}^D$
$-$	$+$	$+$	$c1_{[A]BC}^D$	$c1$ see (6)	$+a1_{B:D}^{4A}$	$+a1_{[0]:BD}^{4A}$
$+$	$-$	$+$	$+a1_{[B]:AC}^D$	$+a1_{[B]:AC}^{4D}$	$+a1_{A:4B}^D$	$+a1_{A:4B}^{4D}$
$-$	$-$	$+$	$+a1_{[C]:AB}^D$	$+a1_{[C]:AB}^{4D}$	$c2_{4AD}^B$	$c2_{4A4D}^B$
\pm	$+$	$-$	$+a1_{A:BC}^{4D}$	—	$+a2_{A:B}^{4D}$	—
\pm	$-$	$-$	$-a1_{A:BC}^D$	—	$-a2_{A:B}^D$	—
total #			7	3	7	3

TABLE 8. Parameters for the double covers.

Parameters. Tables 8 give the types and parameters of the double covers corresponding to all homomorphisms $\pi_1(M) \rightarrow \{\pm 1\}$. The parameters for the orientable double covers ($c1$) of $-a1$ take one of the four forms

$$\begin{aligned}
 (6) \quad & c1_{2C}^{2D} \begin{matrix} 2D \\ 2C+4A \end{matrix} \begin{matrix} B-C-D \\ B-C-D \end{matrix} & c1_{2B}^{2D} \begin{matrix} 2D \\ 2B+4A \end{matrix} \begin{matrix} C-B-D \\ C-B-D \end{matrix} & c1_{2C}^{2B} \begin{matrix} 2B \\ 2C \end{matrix} \begin{matrix} 4A \\ D-B-C \end{matrix} \\
 & \text{(if } B \geq C + D) & \text{(if } C \geq B + D) & \text{(if } D \geq B + C) \\
 & & c1_{C+D-B}^{C+D-B} \begin{matrix} B+D-C \\ B+D-C \end{matrix} \begin{matrix} B+C-D \\ B+C-D+4A \end{matrix} \\
 & & & \text{(otherwise)}
 \end{aligned}$$

and in several other cases, there are two forms, which we abbreviate using the notation

$$(7) \quad [u]:vw = \begin{cases} w - v : 2v & 2v + 4u & \text{if } v \leq w; \\ v - w : 2w & 2w + 4u & \text{if } v \geq w, \end{cases}$$

and the similar notation without a colon.

9. DIAMETERS AND INJECTIVITY RADII

The *covering radius* of a lattice \mathcal{T} is the minimal radius for which the closed balls of that radius centered at points of \mathcal{T} cover the space. It coincides with the *diameter* of the torus R^n/\mathcal{T} , where the diameter of a Riemannian manifold is defined in general to be the maximal distance between any pair of points in it.

The *packing radius* of \mathcal{T} is the maximal radius for which the open balls centered at points of \mathcal{T} are disjoint. In the torus R^n/\mathcal{T} , it becomes the *injectivity radius*, which is defined for every Riemannian manifold to be the maximal radius for which balls of that radius centered at any point of the manifold will embed in the manifold. These are easier to determine:

Injectivity Radii.

Proposition. *The injectivity radius of a platycosm is bounded below by the packing radius of its naming lattice \mathcal{N} . Moreover, these two concepts coincide for 8 of the 10 platycosms.*

Proof. The injectivity radius equals one half of the length of the shortest closed geodesic in the manifold. Every closed geodesic corresponds to a translation, screw motion or glide reflection and its length is exactly the length of the translation vector, screw vector or glide vector, respectively, and all these are by definition in the naming lattice \mathcal{N} . This proves the first assertion.

On the other hand, one can check that the shortest possible vectors of \mathcal{N} do correspond to such ‘geodesic’ vectors in 8 out of the 10 cases, the exceptions being the two ‘negatives’ $-a1$ and $-a2$. \square

We now discuss these two exceptions.

Injectivity radius of $-a1$. Recall that $\mathcal{N} = \langle \mathbf{w}, \mathbf{x}, \mathbf{z} \rangle$, whose conorms and vonorms we display:

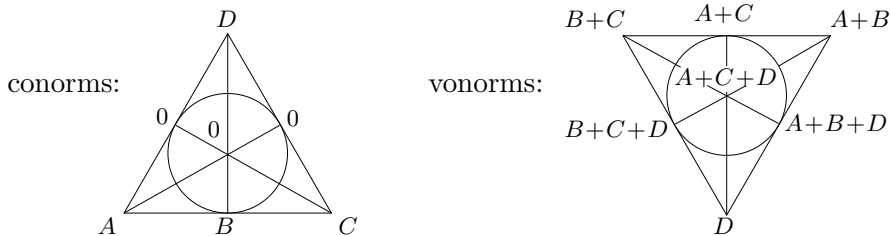


FIGURE 27.

We now classify the geodesic vectors:

kind of vector	vectors	norm of minimal vector
glide vector	$odd \cdot \mathbf{w} + even \cdot \mathbf{x}$	$A + B = N(\mathbf{w})$
	$even \cdot \mathbf{w} + odd \cdot \mathbf{x}$	$A + C = N(\mathbf{x})$
translation vec.	$odd \cdot \mathbf{w} + odd \cdot \mathbf{x} + odd \cdot \mathbf{z}$ $even \cdot \mathbf{w} + even \cdot \mathbf{x} + even \cdot \mathbf{z}$	$B + C + D = N(\mathbf{w} + \mathbf{x} + \mathbf{z})$ $4 \cdot \min(\text{all vonorms})$

seeing that they lie in four cosets of \mathcal{N} in $2\mathcal{N}$. But by vonorm theory (see Appendix II), the minimal norms in these cosets are the numbers in the right column.

So the squared injectivity radius is the minimum of the ten numbers

$$A + B, A + C, A + B + D, 4D, 4(B + C), 4(A + B), 4(A + C), 4(A + B + D), 4(A + C + D), 4(B + C + D),$$

of which those in the second line are dominated. Any of the five numbers in the first line can be the minimum!

Injectivity radius of $-a2$. The vectors corresponding to a letter ‘**d**’ in the figure are of the form $odd \cdot \mathbf{x} + even \cdot \mathbf{w}$. In this way we obtain

letter	vector	minimal vector	norm
d	$odd \cdot \mathbf{x} + even \cdot \mathbf{y}$	\mathbf{x}	A
q	$odd \cdot \mathbf{y}$	\mathbf{y}	B
p	$odd \cdot \mathbf{y} + odd \cdot \mathbf{z}$	$\mathbf{y} + \mathbf{z}$	$B + D$
b	$even \cdot \mathbf{x} + even \cdot \mathbf{y} + even \cdot \mathbf{z}$	(in $2\mathcal{N}$)	$4 \cdot \min(\text{vonorms})$

Hence the answer is $\min(A, B, 4D)$, since the other numbers are dominated by A or B .

For $c1$ the answer is the minimal vonorm — see the end of this section.

For cN_{ABC}^D ($N > 1$), it is generically $\min(B + C, C + A, A + B, D)$. The particular cases are listed in Table 9.

Diameters. We illustrate our method for finding diameters by considering that of the Klein bottle. The solid rectangles in Figure 28 are the Voronoi cells (see Section 11) of the images of \mathbf{p}_0 under Γ . This is an orbit which is also a lattice, so that the rectangles form the *Voronoi tiling* of an *orbit lattice*.

Moreover, this tiling is *translatable* in the sense that it remains a tiling if we move its tiles (say as indicated by the dashed lines) so that their centers form the orbit of an arbitrary other point \mathbf{p}_1 (although the tiles might no longer be Voronoi cells).

It follows that the diameter of the Klein bottle is exactly the circumradius of these rectangles, since the corners of the original rectangles are exactly this distance from \mathbf{p}_0 , and clearly no point can be further than this distance from the generic point \mathbf{p}_1 . The argument proves in general

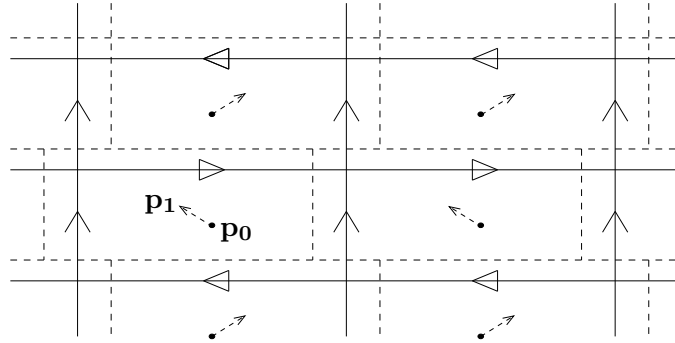


FIGURE 28. Translating the Voronoi cells.

Proposition. *The diameter of a platycosm P is bounded below by the covering radius of any orbit lattice. If P has an orbit lattice whose Voronoi tiling is translatable then its diameter equals the covering radius of that orbit lattice. \square*

The orbit lattice bound R_0 for the diameter of a platycosm P is the maximum of the covering radii of all orbit lattices for P , and we say P has the orbit lattice property if its diameter equals this lower bound. We believe

(The orbit lattice conjecture for platycosms). *All 10 platycosms have the orbit lattice property.*

The proposition establishes this for 7 of the 10 since they have orbit lattices whose Voronoi tilings are translatable. The authors have worked out the orbit lattice bound for the three exceptions, and now summarize the results.

Didicosm. The didicosm $c22^A B C$ has 8 orbit lattices, of just 4 distinct shapes, for which the values of $4R^2$ are:

$$\alpha = A + \frac{(B+C)^2}{\max(B,C)}, \quad \beta = B + \frac{(C+A)^2}{\max(C,A)}, \quad \gamma = C + \frac{(A+B)^2}{\max(A,B)}$$

and

$$\delta = A + B + C + m^2 \cdot \max\left(\frac{1}{A} + \frac{1}{B} + \frac{1}{C} - \frac{2}{m}, 0\right), \quad \text{where } m = \min(A, B, C).$$

Hence the orbit lattice bound is given by $4R_0^2 = \max(\alpha, \beta, \gamma)$, since it can be shown that δ is dominated by any of α, β, γ .

Second amphidicosm. The second amphidicosm $-a2_{A:B}^C$ has infinitely many orbit lattices, of just three different shapes, for which the values of $4R^2$ are the above β, γ, δ . The orbit lattice bound is therefore given by $4R_0^2 = \max(\beta, \gamma)$.

platycosm	squared injectivity radius	squared diameter
$c1_{ABC}^{DEF}$	the minimal vonorm — see below	see Section 10
$c2_{ABC}^D$	$\min(B + C, C + A, A + B, D)$	$\frac{(B+C)(C+A)(A+B)}{4(BC+CA+AB)} + \frac{D}{4}$
$c3_{AAA}^D$	$\min(2A, D)$	$\frac{2}{3}A + \frac{D}{4}$
$c4_{AA}^D$	$\min(A, D)$	$\frac{1}{2}A + \frac{D}{4}$
$c6_{AAA}^D$	$\min(2A, D)$	$\frac{2}{3}A + \frac{D}{4}$
$c22^{ABC}$	$\min(A, B, C)$	$\geq \frac{1}{4} \max(\alpha, \beta, \gamma)$
$+a1_{A:BC}^D$	$\min(A + B, B + C, A + C, D)$	$\frac{(B+C)(C+A)(A+B)}{4(BC+CA+AB)} + \frac{D}{4}$
$-a1_{A:BC}^D$	$\min(A + B, A + C, B + C + D, 4D, 4(B + C))$	see text
$+a2_{A:B}^C$	$\min(A, B, C)$	$\frac{1}{4}(A + B + C)$
$-a2_{A:B}^C$	$\min(A, B, 4C)$	$\geq \frac{1}{4} \max(\beta, \gamma)$

TABLE 9. Injectivity radii and diameters. Here

$$\alpha = A + \frac{(B+C)^2}{\max(B,C)}, \beta = B + \frac{(C+A)^2}{\max(C,A)}, \gamma = C + \frac{(A+B)^2}{\max(A,B)}.$$

Second amphiocosm. The hardest case is $-a1_{A:BC}^D$, which has just 2 distinct shapes of orbit lattices. For the first of these,

$$(8) \quad 4R^2 = \begin{cases} I & \text{if } C \geq D, \\ \max(II, V) & \text{if } C \leq D \leq A + C, B + C, \\ \max(III, V) & \text{if } B + C \leq D, B \leq A, \\ \max(IV, V) & \text{if } B + C \leq D, B \geq A, \end{cases}$$

where

$$\begin{aligned} I &= A + B + 4D + (A + B)(D - C)^2/\Omega \\ II &= A + B + 4C + (A + B + 4C)(D - C)^2/\Omega \\ III &= 2B + 2C + D + (B + C)^2/D + (B + C)(B - A)^2/\Omega \\ IV &= 2A + 2C + D + (A + C)^2/D + (A + C)(B - A)^2/\Omega \\ V &= A + B + 2C + C^2/D \end{aligned}$$

where $\Omega = BC + CA + AB$. Equivalently, it can be shown to be the minimum of the four expressions in (8), which may be rewritten as

$$\max\left(\min(I, II, III, IV), \min(I, V)\right).$$

For the second orbit lattice, $4R^2$ is given by the similar expression

$$\max\left(\min(I', II', III', IV'), \min(I', V')\right).$$

found by interchanging B and C .

Therefore the orbit lattice bound is given by

$$4R_0^2 = \max \left(\min(I, II, III, IV), \min(I, V), \min(I', II', III', IV'), \min(I', V') \right).$$

10. SOME FORMULAE FOR TOROCOSMS AND LATTICES

Many functions of a 3-dimensional lattice (or its associated torocosm) can be expressed as symmetrical functions of all 7 conorms. For instance, the squared packing or injectivity radius is the minimal vonorm, and of course the typical conorm is just the sum of conorms not on a given line, so the lattice $\Lambda_{ABC}^{DEF G}$ has the conorms and vonorms of Figure 29. The G conorm is not necessarily the zero

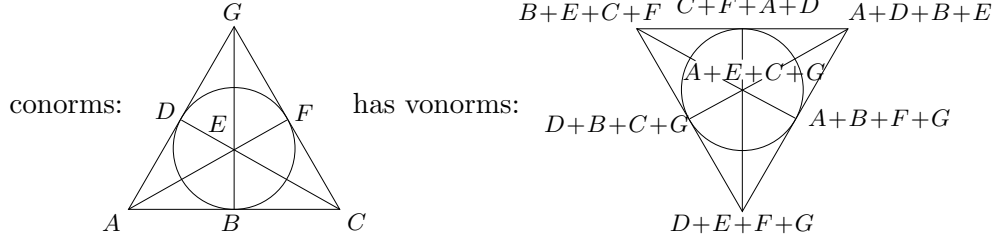


FIGURE 29.

one. If it is, the squared injectivity radius (of $c1_{ABC}^{DEF}$) simplifies to

$$\min (B+E+C+F, C+F+A+D, A+D+B+E, D+B+C, A+E+C, A+B+F, D+E+F).$$

The determinant of this lattice (which is the squared volume of the corresponding torocosm) is the sum of the conorm products over all 28 triangles in the conorm plane. When G is zero, 12 of those products vanish, and the determinant simplifies to

$$\Delta = (A+D)(BE+CF)+(B+E)(CF+AD)+(C+F)(AD+BE)+DBC+AEC+ABF+DEF.$$

The actual length of the edge in Figure 30 marked with a given conorm x is

$$(9) \quad \frac{x}{\Delta} \sqrt{\frac{\partial \Delta}{\partial x}}$$

where $\frac{\partial \Delta}{\partial x}$ denotes the formal derivative of the above expression for Δ with respect to the variable x . It is easy to check that (9) can vanish only when x does.

Another useful expression is Δ' , the sum of conorm products over the complements of all triangles; when $G = 0$ this simplifies to

$$\Delta' = AD(B+E)(C+F) + BE(C+F)(A+D) + CF(A+D)(B+E),$$

since now 16 of the products vanish. It can be shown that the covering radius is given (when $G = 0$) by

$$(10) \quad 4R^2 = A + B + C + D + E + F - \frac{\Delta' + 4 \cdot \min(BECF, CFAD, ADBE)}{\Delta}$$

Finally, we remark that the lattice Λ_{abc}^{defg} dual to Λ_{ABC}^{DEF} has conorms given by

$$\begin{aligned} a\Delta &= AD - m, & d\Delta &= AE + AF + EF + m, \\ b\Delta &= BE - m, & e\Delta &= BD + BF + DF + m, \\ c\Delta &= CF - m, & f\Delta &= CD + CE + DE + m, \\ & & g\Delta &= AB + AC + BC + m, \end{aligned}$$

where $m = \min(AD, BE, CF)$.

11. THE BRAVAIS-VORONOI CLASSES

Voronoi classification of lattices. The points of space that are closer to one particular lattice point than to any other constitute the *Voronoi cell* of that point. In [Co2] conorms were used to give a simple derivation of Voronoi's classification of lattices by the topological type of their Voronoi cells.

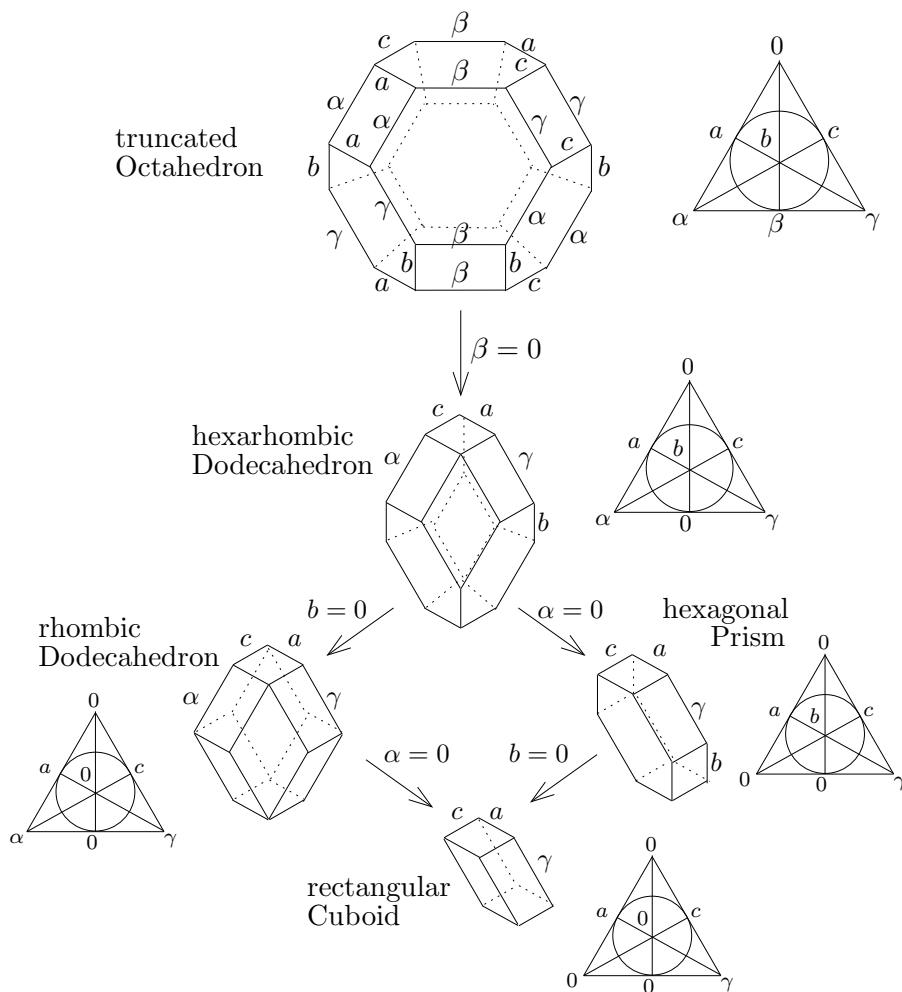


FIGURE 30. The shape of the Voronoi cell.

The generic Voronoi cell is a truncated octahedron as in Figure 30, adapted from [Co2]. The six families of parallel edges correspond to its six non-zero conorms. When any conorm vanishes, the corresponding edges shrink to points, changing the Voronoi cell into one of the four other shapes: a hexarhombic dodecahedron, a rhombic dodecahedron, a hexagonal prism, or a rectangular cuboid (see Figure 30).

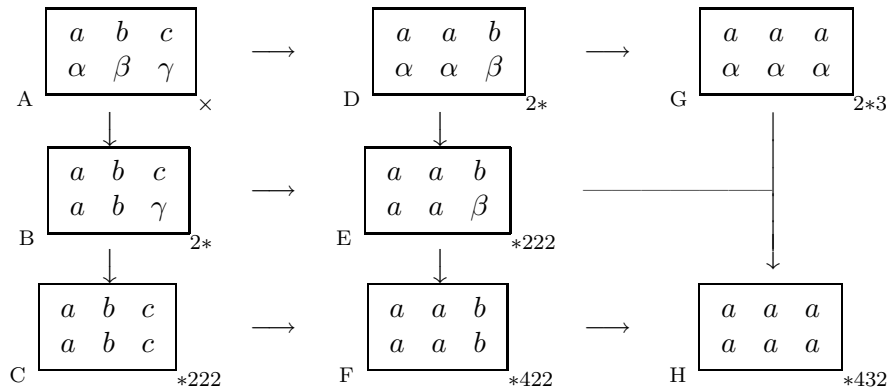
Each of these figures has antipodal symmetry. Any other topological symmetry will become a metrical one provided certain conorms are equal. Since the possible topological symmetries depend on which conorms vanish, we have found it convenient to adjust the lettering to display this more clearly. The cases are:

lattice	(abbreviating)	effect of symmetries on the conorms
Λ_{ABC}^{DEF}		Make two of the interchanges $A \leftrightarrow D, B \leftrightarrow E, C \leftrightarrow F$. Bodily permute the three columns.
$\Lambda_{CD:E}^{AB}$	Λ_{CDE}^{ABO}	Make either of the interchanges $A \leftrightarrow B, C \leftrightarrow D$. Bodily permute these two couples.
Λ_{CD}^{AB}	Λ_{CDO}^{ABO}	Permute A, B, C, D in any way.
Λ_{ABC}^D	Λ_{ABC}^{DOO}	Permute A, B, C in any way.
Λ^{ABC}	Λ_{OOO}^{ABC}	Permute A, B, C in any way.

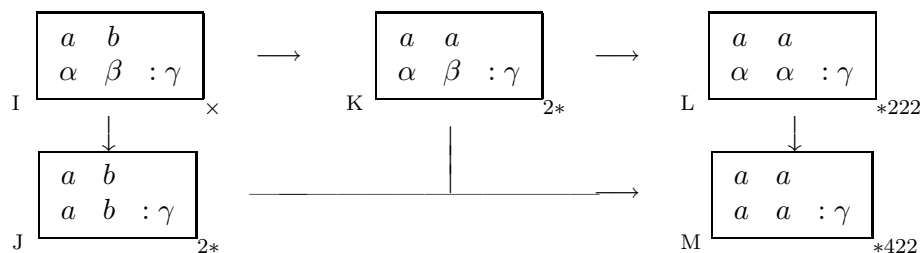
Deducing the Bravais classification. The arrows in the following figures show how certain equalities between conorms permit additional metrical symmetries (the arrows being downward or rightward according as the symmetries move numbers within their columns or across columns). They show that 3-dimensional lattices belong to just 24 ‘BraVo’ (Bravais-Voronoi) classes, where we say that two lattices are in the same BraVo class just if each can be continuously deformed into the other while keeping all its symmetries and without changing the topological shape of its Voronoi cell.

Below each conorm array is a naming letter A,B,...,X, and the orbifold notation for the corresponding point group.

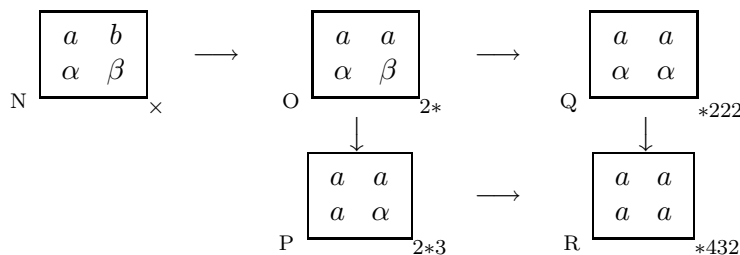
Truncated Octahedron (tO).



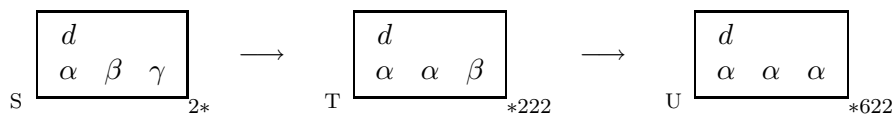
Hexarhombic Dodecahedron (hD).



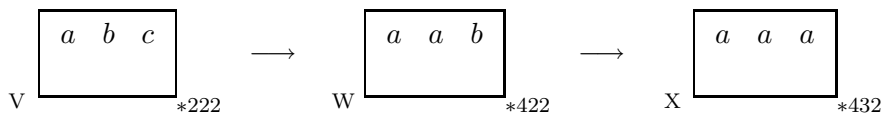
Rhombic Dodecahedron (rD).



Hexagonal Prism (hP).



Rectangular Cuboid (rC).



The easiest proof that there are just 14 Bravais classes is to see how certain continuous variations link the 24 BraVo classes. For example, take the lattice $\Lambda_{\alpha\alpha\alpha}^{aaa}$ (case G) and vary α until it becomes a small negative number $-\epsilon$, forcing us to renormalize the conorms as in Figure 31.

Then the new lattice has shape Λ_{ab}^{aa} (case P), showing that cases G and P are in the same Bravais class. To obtain the exact partition into Bravais classes one merely has to vary the parameters like this in all possible ways for which the new lattice has no more symmetries than the old one¹³. Similarly, making b negative in case F leads to case M. All other identifications can be achieved just by making some conorms vanish, as in Figure 32.

This gives Table 10, whose last column gives the “symmetry factors” by which the sizes of the isometry groups have been increased.

To prove this list is complete, it suffices to show that any other cases with the same group are in distinct Bravais classes, which follows from the fact that each of E,H,R,S,T,U,V,W,X is in a Bravais class of its own. Why is this? For

¹³although at isolated intermediate times the symmetry might have been larger, as it was in this case when $\alpha = 0$

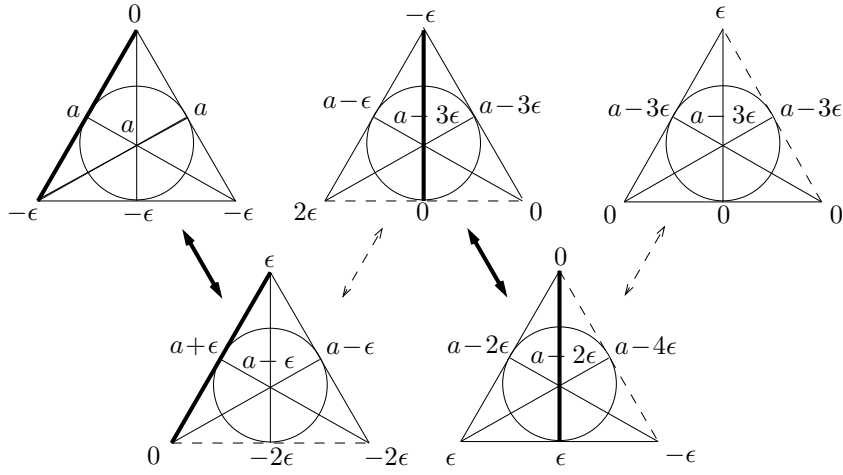


FIGURE 31.

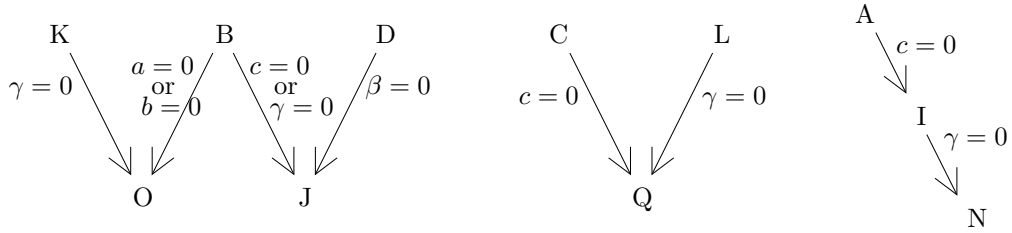


FIGURE 32.

H,R,V,W,X no parameter can pass through 0 without the lattice degenerating. The same is true for the parameter a in E and d in S,T,U. For E this leaves essentially only the normalization of $\begin{pmatrix} a & a & \epsilon \\ a & a & \beta \end{pmatrix}$ to $\begin{pmatrix} a - \epsilon & a - \epsilon & \epsilon \\ a - \epsilon & a - \epsilon & \beta + \epsilon \end{pmatrix}$, which is again in case E. The argument for S,T,U is even easier, and completes the proof of the Bravais classification.

Bravais types for the other platycosms. For the remaining helicosms cN_{ABC}^D the Bravais classification reduces to that of the 2-dimensional lattice Λ_{ABC} , since D can be varied independently of A, B, C . Thus $c2$ has five Bravais types:

$$c2_{ABC}^D \longrightarrow c2_{AAB}^D \longrightarrow c2_{AAA}^D, \quad c2_{AB}^D \longrightarrow c2_{AA}^D$$

where $c2_{AB}^D$ means $c2_{AB0}^D$, and $c3, c4, c6$ just one each

$$c3_{AAA}^D, c4_{AA}^D, c6_{AAA}^D.$$

For the didicosm $c22$, the classification is just that of the rectangular 3-dimensional lattice Λ^{ABC} :

$$c22^{ABC} \longrightarrow c22^{AAB} \longrightarrow c22^{AAA}.$$

<i>Voronoi classes</i>					<i>Bravais classes</i>	
tO	hD	rD	hP	rC	crystallographic name	symmetry factor
A	I	N			Triclinic	1
BD	JK	O			base-centered Monoclinic	2
C	L	Q			body-centered Orthorhombic	4
E					face-centered Orthorhombic	4
F	M				body-centered Tetragonal	8
G		P			Rhombohedral (or Trigonal)	6
H					body-centered Cubic (bcc)	24
		R			face-centered Cubic (fcc)	24
			S		primitive Monocline	2
			T		base-centered Orthorhombic	4
			U		Hexagonal	12
				V	Orthorhombic	4
				W	primitive Tetragonal	8
				X	primitive Cubic	24

TABLE 10. How the 24 BraVo classes correspond to the 5 Voronoi and 14 Bravais classes.

For the two amphicosms $\pm a1_{A:BC}^D$, the Bravais classification reduces to that of the 2-dimensional lattice Λ_{ABC} , but taking into account the distinguished rôle of A :

$$\begin{aligned}
 +a1_{A:BC}^D &\longrightarrow +a1_{A:BB}^D, & +a1_{:BC}^D &\longrightarrow +a1_{:BB}^D, & +a1_{A:B}^D, \\
 -a1_{A:BC}^D &\longrightarrow -a1_{A:BB}^D, & -a1_{:BC}^D &\longrightarrow -a1_{:BB}^D, & -a1_{A:B}^D,
 \end{aligned}$$

where, of course, $\pm a1_{A:B}^D$ and $\pm a1_{:BC}^D$ abbreviate $\pm a1_{A:B0}^D$ and $\pm a1_{0:BC}^D$ respectively.

Finally, each of the amphidicosms $\pm a2_{A:B}^D$ forms a single Bravais type since all three parameters are distinguishable. We conclude:

The numbers of Bravais types of platycosms are

14	5	1	1	1	3	5	5	1	1	(total 37)
for	$c1$	$c2$	$c3$	$c4$	$c6$	$c22$	$+a1$	$-a1$	$+a2$	$-a2$

APPENDIX I: WHY THERE ARE JUST 10 PLATYCOSMS

Why are there exactly 10 compact platycosms? We sketch a proof of this to make our paper complete. The proof is outlined in Figure 33 and the accompanying explanations (i)–(vi). We quote Bieberbach’s theorem that the subgroup of translations has finite index.

(i) When there are screw motions there is a

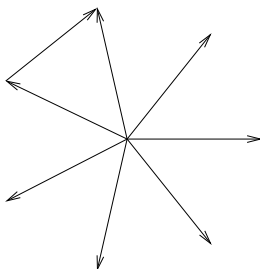
Splitting Lemma. *If \mathbf{v} is the smallest screw vector in a given direction, say vertical, then the translation lattice \mathcal{T} decomposes as $\langle N\mathbf{v} \rangle \oplus \mathcal{T}'$, where N is the period of the corresponding screw motion σ .*

Proof. It suffices to prove that there is no translation τ whose vertical part $c\mathbf{v}$ is strictly between 0 and $N\mathbf{v}$. But then $\sigma\tau^{-1}$ if $0 < c < 1$, or $\tau\sigma^{-m}$ if $m < c < m + 1$ ($m = 1, \dots, N - 1$) would be a vertical screw motion with shorter vector than \mathbf{v} . \square

(ii) If all screw vectors are parallel we have a cyclic point group whose order N is the least common multiple of their periods and which acts on the 2-dimensional lattice \mathcal{T}' . Obviously Γ is generated by the shortest screw motion of this period together with the translations of \mathcal{T}' . The identification with $c2, c3, c4$ or $c6$ follows from the well known lemma:

Barlow's Lemma. *If a rotation of order N fixes a 2-dimensional lattice \mathcal{T}' , then $N = 1, 2, 3, 4, 6$.*

Proof. Apply the rotation to a minimal non-zero vector of the lattice. We obtain a 'star' of N vectors, the difference of adjacent members of which will be a shorter



vector if $N \geq 7$. A rotation of order 5 would combine with negation to produce one of order 10. \square

(iii) Two non parallel screw motions σ_1 and σ_2 would make \mathcal{T} decompose in two ways, say $\langle \mathbf{v}_1 \rangle \oplus \mathcal{T}_1 \cong \langle \mathbf{v}_2 \rangle \oplus \mathcal{T}_2$, showing immediately that \mathbf{v}_1 and \mathbf{v}_2 are orthogonal. If σ_i had a period other than 2, then σ_j and $\sigma_j^{\sigma_i}$ would not be orthogonal. Finally, if σ_1 and σ_2 are orthogonal and of period 2, then $\sigma_1\sigma_2$ is a screw motion in the direction of \mathbf{v}_3 orthogonal to \mathbf{v}_1 and \mathbf{v}_2 . These together with the translations must generate Γ , and can be identified with the X, Y, Z of $c22$.

(iv) Any glide reflection maps to a reflection through the origin when ignore translations. The product of two of them is therefore a translation or a screw motion since the product of two reflections through \mathbf{o} is the identity or a non-trivial rotation according as their planes are parallel or not.

(v) If all glide reflections are in parallel planes — call them basal — the point group has order 2, so Γ is generated by a single glide reflection, together with its translations. We resolve any translation vector into basal and perpandal parts $\mathbf{v}_1 + \mathbf{v}_2$, and see that since τ takes this to $\mathbf{v}_1 - \mathbf{v}_2$, $2\mathbf{v}_2$ is also a translation vector. If \mathbf{v}_2 itself (and so \mathbf{v}_1) is a translation vector, then the translation lattice \mathcal{T} decomposes into its basal and perpandal parts, leading to $+a1$. Otherwise, adjoining the translation through \mathbf{v}_2 embeds our platycosm in a copy of $+a1$, and easily identifies the original platycosm with $-a1$.

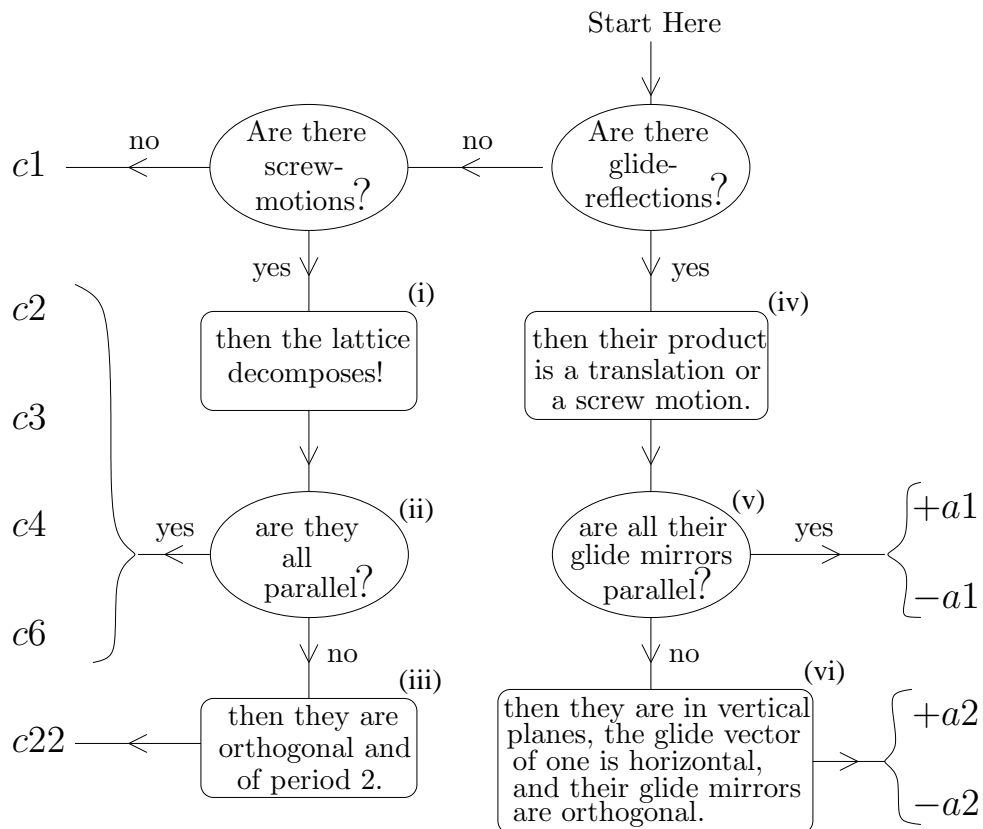


FIGURE 33. Guide to the proof.

(vi) If two glide reflections g, g' have non-parallel planes intersecting in a line we will call vertical, then their product will be a screw motion s whose screw vector \mathbf{v} will be vertical. We choose things so that \mathbf{v} is as short as possible. Then we can multiply by a power of s to reduce g until the vertical component of its glide vector $\lambda\mathbf{v}$ has $|\lambda| \leq \frac{1}{2}$. But then λ must be 0 since g^2 is a translation and by the Splitting Lemma its vertical component must be a multiple of $N\mathbf{v}$, where $N \geq 2$ is the period of s .

The glide vector of the new g' (defined by $gg' = s$) will have the same vertical component \mathbf{v} as s . But now the translation vector $(g')^2$ has vertical component $2\mathbf{v}$, showing (by the Splitting Lemma) that s must have period 2, from which it follows that the planes of g and g' are orthogonal.

We can now see that the translation lattice is generated by 3 orthogonal translations, say $(x, y, z) \mapsto (x + a, y, z), (x, y + b, z), (x, y, z + c)$. We can also see that the point group has order 4, i.e. that g, g' , together with translations, must generate Γ . For if not, there would be a glide mirror not parallel to either of those of g, g' , and so perpendicular to both, by the previous paragraph. But then

the product of the corresponding glide reflection with s would have the form

$$(x, y, z) \mapsto (\text{constant} - x, \text{constant} - y, \text{constant} - z),$$

which fixes a point. In these coordinates

$$\begin{aligned} s &: (x, y, z) \rightarrow (-x, -y, z + \frac{1}{2}c) \\ g &: (x, y, z) \rightarrow (x + \frac{1}{2}a, \lambda b - y, z) \end{aligned}$$

where we may take $0 \leq \lambda < 1$ by compounding g with translations. From these we find

$$\begin{aligned} g' = g^{-1}s &: (x, y, z) \rightarrow (\frac{1}{2}a - x, y - \lambda b, z + \frac{1}{2}c) \\ (g')^2 &: (x, y, z) \rightarrow (x, y - 2\lambda b, z + c) \end{aligned}$$

showing that 2λ must be an integer, so either $\lambda = 0$, which gives $+a2$; or $\lambda = \frac{1}{2}$, which gives $-a2$. In the former case, our screw vector $(0, 0, \frac{1}{2}c)$ is also a glide vector (of g') — in the latter case, no screw vector is a glide vector.

APPENDIX II: CONORMS OF LATTICES

Introduction. The conorms of a lattice \mathcal{L} are certain numbers that are determined by \mathcal{L} (up to equivalence) and return the compliment by determining \mathcal{L} , at least in low dimensions. More precisely \mathcal{L} has a *conorm function* defined on *conorm space*, which is a finite set that has the structure of a projective $(n - 1)$ -dimensional space over the field of order two. At least for $n \leq 4$, two n -dimensional lattices \mathcal{L} and \mathcal{L}' are isometric if and only if there is an isomorphism between their conorm spaces that takes one conorm function to the other.

The theory in low dimensions is greatly simplified by the observation that for $n \leq 3$ every lattice has an *obtuse superbase*, which implies in particular that the conorms are ≥ 0 . A *superbase* for an n -dimensional lattice \mathcal{L} is an $(n + 1)$ -tuple $\{\mathbf{v}_0, \mathbf{v}_1, \dots, \mathbf{v}_n\}$ of vectors that generate \mathcal{L} and sum to zero. It is *obtuse* if all inner products $\mathbf{v}_i \cdot \mathbf{v}_j$ of distinct vectors are non-positive (and *strictly obtuse* if they are strictly negative). For a lattice with an obtuse superbase, it can be shown that the conorms are the negatives of the inner products of pairs of distinct superbase vectors, supplemented by zeros. (If $n \geq 4$ other things can happen; a lattice may not have an obtuse superbase, and some conorms may be strictly negative.)

For $n = 0$, *conorm space is empty*, so there are no conorms.

For $n = 1$, *conorm space is a single point*, and there is one strictly positive conorm A . We represent this by the picture $\overset{A}{\bullet}$; it means that the lattice has an obtuse suberbase $\{\mathbf{v}, -\mathbf{v}\}$ with Gram-matrix $\begin{bmatrix} A & -A \\ -A & A \end{bmatrix}$; equivalently a base $\{\mathbf{v}\}$ with Gram-matrix $[A]$.

For $n = 2$, conorm space is a 3-point projective line, and the 3 conorms A, B, C are non-negative. We represent this by the picture $\bullet \xrightarrow{A} \bullet \xrightarrow{B} \bullet \xrightarrow{C}$; it means that the lat-

tice has an obtuse superbase $\{\mathbf{v}_0, \mathbf{v}_1, \mathbf{v}_2\}$ with matrix $\begin{bmatrix} B+C & -C & -B \\ -C & C+A & -A \\ -B & -A & A+B \end{bmatrix}$,

or equivalently a base $\{\mathbf{v}_0, \mathbf{v}_1\}$ with matrix $\begin{bmatrix} B+C & -C \\ -C & C+A \end{bmatrix}$.

For $n = 3$, conorm space is the 7-point “Fano plane”, represented by Figure 34. The superbase has Gram-matrix

$$\begin{bmatrix} p_{0|123} & -p_{12} & -p_{13} & -p_{01} \\ -p_{12} & p_{1|023} & -p_{23} & -p_{02} \\ -p_{13} & -p_{23} & p_{2|013} & -p_{03} \\ -p_{01} & -p_{02} & -p_{03} & p_{3|012} \end{bmatrix},$$

where $p_{ij} = p_{ji} \geq 0$, $p_{i|jkl} := p_{ij} + p_{ik} + p_{il}$, and the minimal conorm is 0.

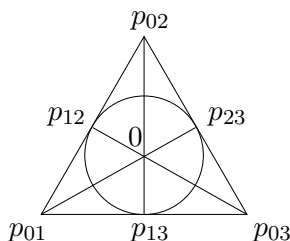


FIGURE 34. A Fano plane with $p_{01}, p_{02}, p_{03}, p_{12}, p_{13}, p_{23}, 0$ in the usual arrangement.

The sum of the four conorms not on a given line in Fig. 34 is a *vonorm*, which can be defined either as the norm of a Voronoi vector, or as the minimal norm of any vector in a non-trivial coset of \mathcal{L} in $2\mathcal{L}$.

Putative conorms and the reduction algorithm. A 3-dimensional lattice has many systems of “putative conorms” in addition to its unique system of actual conorms, for instance the numbers obtained by arranging 0 and the negatives $p_{ij} := -v_i \cdot v_j$ of the inner products of distinct members of *any* superbase on a Fano plane in the manner of Figure 34. If the putative conorms are all non-negative, they will be the actual conorms. Otherwise, the following algorithm quoted from [Co2] and [CoS] will produce the latter.

Select a ‘working line’ that contains both a 0 conorm and a negative one, say $-\epsilon$. Then we transform to an improved system of putative conorms by adding ϵ to the 3 conorms on the working line, and subtracting ϵ from the 4 conorms off this line. If the improved system still has a negative conorm, we can define a new working line and repeat the procedure. A finite number of repetitions will suffice to produce the actual conorms.

As an example Figure 35 finds the conorms for the lattice whose Gram-matrix with respect to a suitable base $\mathbf{v}_1, \mathbf{v}_2, \mathbf{v}_3$ is $\begin{bmatrix} 2 & 1 & 1 \\ 1 & 3 & 1 \\ 1 & 1 & 4 \end{bmatrix}$. The Gram-matrix for the superbase $\mathbf{v}_1, \mathbf{v}_2, \mathbf{v}_3, -\mathbf{v}_1 - \mathbf{v}_2 - \mathbf{v}_3$ is $\begin{bmatrix} 2 & 1 & 1 & -4 \\ 1 & 3 & 1 & -5 \\ 1 & 1 & 4 & -6 \\ -4 & -5 & -6 & 15 \end{bmatrix}$ (found by making each row and column sum to 0), which leads to the putative conorms of Figure 35(a). Transforming this using the working line indicated on it, we obtain Figure

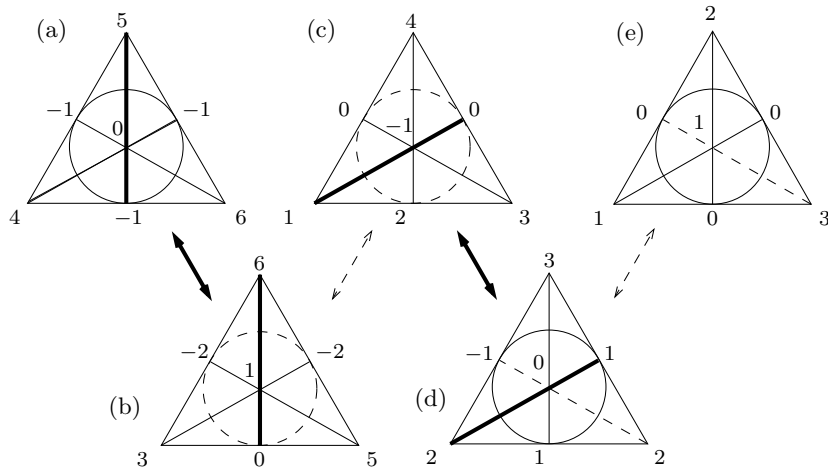


FIGURE 35.

35(b), and we proceed from this in a similar way to Figures 35(c), 35(d), 35(e), the last of which gives the actual conorms. The reader might like to verify that another choice of working line yields the same conorm function.

For a 2-dimensional lattice with putative conorms A, B, C there is a similar algorithm. We select a ‘working point’ at which there is a negative conorm, say $-\epsilon$, and transform by adding 2ϵ to this conorm and subtracting 2ϵ from the other two conorms. Thus $\begin{array}{ccc} -3 & 5 & 10 \\ \bullet & \bullet & \bullet \end{array}$ transforms through $\begin{array}{ccc} 3 & -1 & 4 \\ \bullet & \bullet & \bullet \end{array}$ to $\begin{array}{ccc} 1 & 1 & 2 \\ \bullet & \bullet & \bullet \end{array}$.

APPENDIX III: DICTIONARY OF NAMES AND NOTATIONS

The purpose of this appendix is to give to readers who have met with a platycosm in some other notation a way to recognize it quickly. Some of the notations are for the corresponding space groups. We take the translations of these in the form

$$(x, y, z) \rightarrow (x + l, y + m, z + n) \quad (l, m, n \in \mathbb{Z})$$

and use the additional generators given in the last column (in which the coordinates are not necessarily orthonormal). These are taken from CARAT (cf. [CiS]), which has such information up to dimension 6.

our name	symbol	other names	Wolf
torocosm	$c1$	3-torus	\mathcal{G}_1
dicosm	$c2$	half turn space	\mathcal{G}_2
tricosm	$c3$	one-third turn space	\mathcal{G}_3
tetracosm	$c4$	quarter turn space	\mathcal{G}_4
hexacosm	$c6$	one-sixth turn space	\mathcal{G}_5
didicosm	$c22$	Hantzsche-Wendt space	\mathcal{G}_6
first ampicosm	$+a1$	Klein bottle times circle	\mathcal{B}_1
second ampicosm	$-a1$		\mathcal{B}_2
first amphidicosm	$+a2$		\mathcal{B}_3
second amphidicosm	$-a2$		\mathcal{B}_4

TABLE 11. Names and notations for platycosms.

symbol	[CDHT]	internatl. no. name	non-translation generators
$c1$	(\circ)	1. $P1$	—
$c2$	$(2_1 2_1 2_1 2_1) = (\bar{\times} \bar{\times})$	4. $P2_1$	$(-x, -y, z + 1/2)$
$c3$	$(3_1 3_1 3_1)$	144. $P3_1$ 145. $P3_2$	$(-x - y, x, z + 1/3)$
$c4$	$(4_1 4_1 2_1)$	76. $P4_1$ 78. $P4_3$	$(-y, x, z + 1/4)$
$c6$	$(6_1 3_1 2_1)$	169. $P6_1$ 170. $P6_5$	$(x + y, -x, z + 1/6)$
$c22$	$(2_1 2_1 \bar{\times})$	19. $P2_1 2_1 2_1$	$(-x, y + 1/2, -z + 1/2)$ $(x + 1/2, -y, -z)$
$+a1$	$(\bar{\circ}_0) = (*:*) = (\times \times_0)$	7. Pc	$(x + 1/2, y, -z)$
$-a1$	$(\bar{\circ}_1) = (*:\times) = (\times \times_1)$	9. Cc	$(x + 1/2, z, y)$
$+a2$	$(2_1 2_1 *:*) = (\bar{*}:\bar{*}:) = (\bar{\times} \times_0)$	29. $Pca2_1$	$(-x, y, z + 1/2)$ $(x + 1/2, -y, z)$
$-a2$	$(2_1 2_1 \times) = (*:\bar{\times}) = (\bar{\times} \times_1)$	33. $Pa2_1$	$(-x, y + 1/2, z + 1/2)$ $(x + 1/2, -y, z)$

TABLE 12. Notations for space groups.

The two international numbers and names given in the three metachiral cases correspond to the two orientations.

The infinite — or non-compact — platycosms were systematically treated probably for the first time in [Wo] p.123, with the symbols indicated in the corresponding column of the following table:

our name	symbol	Wolf
Euclidean Space	EUC	\mathcal{E}
Circular Product space	$CPS_A(\theta)$	\mathcal{S}_1^θ
Circular Möbius space	CMS_A	\mathcal{S}_2
Toroidal Product space	TPS_{ABC}	\mathcal{T}_1
Toroidal Möbius space	$TMS_{A:B:C}$	\mathcal{T}_2
Kleinian Product space	KPS_B^A	\mathcal{K}_2
chiral Kleinian Möbius space	$+KMS_B^A$	\mathcal{K}_1
achiral Kleinian Möbius space	$-KMS_B^A$	\mathcal{K}_3

TABLE 13. Infinite platycosms.

REFERENCES

- [Ch] CHARLAP, L.S., Bieberbach groups and flat manifolds. *Universitext. Springer-Verlag, New York*, 1986.
- [ChV] CHARLAP, L. S.; VASQUEZ, A. T., Compact flat riemannian manifolds. III. The group of affinities. *Amer. J. Math.* **95** (1973), 471–494.
- [CiS] CID, C.; SCHULZ, T., Computation of Five and Six dimensional Bieberbach groups. *Experiment Math.* **10** (2001), 109–115.
- [Co1] CONWAY, J.H., The orbifold notation for surface groups. In *Groups, combinatorics and geometry* (Durham, 1990), 438–447, London Math. Soc. Lecture Note Ser., 165, Cambridge Univ. Press, Cambridge, 1992.
- [Co2] CONWAY, J.H. (with the assistance of F.Y.C. FUNG), The sensual (quadratic) form, *Carus Mathematical Monographs*, **26** Mathematical Association of America, Washington, DC (1997).
- [CDHT] CONWAY, J.H.; DELGADO FRIEDRICH, O.; HUSON, D.H.; THURSTON, W.P., On three-dimensional space groups. *Beiträge Algebra Geom.* **42** (2001), no. 2, 475–507.
- [CoS] CONWAY, J.H.; SLOANE, N.J.A., Low-dimensional lattices. VI. Voronoi reduction of three-dimensional lattices, *Proc. Roy. Soc. London Ser. A* **436** (1992), no. 1896, 55–68.
- [DR] DOYLE, P.G.; ROSSETTI, J.P., Tetra and Didi, the cosmic spectral twins. *Preprint*.
- [E] EFSTATHIOU, G., Is the Low CMB Quadrupole a Signature of Spatial Curvature? Submitted to *MNRAS*, arXiv:astro-ph/0303127.
- [HS] HAJIAN, A.; SOURADEEP, T., Statistical Isotropy of CMB and Cosmic Topology. Submitted to *Phys. Rev. Lett.*, arXiv: astro-ph/0301590.
- [HW] HANTZSCHE W.; WENDT H., Dreidimensionale euklidische Raumformen. *Math. Annalen.* **110** (1934–35), 593–611.
- [Hi] HILLMAN, J.A., Flat 4-manifold groups. *New Zealand J. Math.* **24** (1995), no. 1, 29–40.
- [LSW] LUMINET, J.P.; STARKMAN, G.D.; WEEKS, J.R., Is Space Finite? *Scientific American* (1999), no. April, 90–97.
- [MS] MALFAIT, W.; SZCZEPAŃSKI, A., The structure of the (outer) automorphism group of a Bieberbach group. *Compositio Math.* **136** (2003), no. 1, 89–101.
- [No] NOWACKI, W., Die euklidischen, dreidimensionalen, geschlossenen und offenen Raumformen. *Comm. Math. Helv.* **7** (1934), 81–93.
- [NYT] DENNIS OVERBYE, Universe as Doughnut: New Data, New Debate. *New York Times* March 11, 2003.
- [RC] ROSSETTI, J.P.; CONWAY, J.H., Hearing the Platycosms. *Preprint*.
- [Spe] SPERGEL, D.N.; ET AL., First Year Wilkinson Microwave Anisotropy Probe (WMAP) Observations: Determination of Cosmological Parameters. To appear in *The Astrophysical Journal*, astro-ph/0302209.

- [TOH] TEGMARK, M.; DE OLIVEIRA-COSTA, A.; HAMILTON, A., A high resolution foreground cleaned CMB map from WMAP. arXiv:astro-ph/0302496.
- [Th] THURSTON, W.P., Three-dimensional geometry and topology. Vol. 1. *Edited by Silvio Levy. Princeton Mathematical Series, 35. Princeton University Press, Princeton, NJ, 1997.*
- [URLW] UZAN, J.-P.; RIAZUELO, A.; LEHOUCQ, R; WEEKS, J., Cosmic microwave background constraints on multi-connected spherical spaces. Submitted to *Phys.Rev.Lett.*, arXiv:astro-ph/0303580.
- [We1] WEEKS, J.R. The shape of space. *Second edition. Monographs and Textbooks in Pure and Applied Mathematics, 249. Marcel Dekker, Inc., New York, 2002.*
- [We2] WEEKS, J.R. Real-Time Rendering in Curved Spaces. *IEEE Computer Graphics and Applications* **22** (2002), no 6, 90–99.
- [Wo] WOLF, J.A., Spaces of constant curvature, *Fifth edition. Publish or Perish, Inc., Houston, TX, 1984.*
- [Zi] ZIMMERMANN, B., On the Hantzsche-Wendt manifold. *Monatsh. Math.* **110** (1990), no. 3-4, 321–327.

DEPARTMENT OF MATHEMATICS, PRINCETON UNIVERSITY, FINE HALL, PRINCETON, NJ 08544, USA.

E-mail address: `conway@math.princeton.edu`

FAMAF(CIEM), UNIVERSIDAD NACIONAL DE CÓRDOBA, CIUDAD UNIVERSITARIA, 5000-CÓRDOBA, ARGENTINA. (VISITING PRINCETON UNIVERSITY).

E-mail address: `rossetti@mate.uncor.edu`, `rossetti@math.princeton.edu`

